Plant Biotechnology Journal
Open Access

Plant Biotechnology Journal (2025) **23**, pp. 2018–2033 doi: 10.1111/pbi.70015

TaWUS-like-5D affects grain weight and filling by inhibiting the expression of sucrose and trehalose metabolism-related genes in wheat grain endosperm

Hongxia Liu[1,*], Tian Li[1], Jian Hou[1], Xiaotong Yin[1], Yuquan Wang[1], Xuemei Si[1], Shoaib Ur Rehman[1], Lei Zhuang[1], Weilong Guo[2], Chenyang Hao[1,*] and Xueyong Zhang[1,*]

[1]*State Key Laboratory of Crop Gene Resources and Breeding, Institute of Crop Sciences, Chinese Academy of Agricultural Sciences (CAAS), Beijing, China*
[2]*Frontiers Science Center for Molecular Design Breeding, China Agricultural University, Beijing, China*

Received 28 October 2024;
revised 6 January 2025;
accepted 7 February 2025.
**Correspondence* (Tel+86 1082105826; fax +86 1082106695; email liuhongxia02@caas.cn (H.X.L.); haochenyang@caas.cn (C.Y.H.); zhangxueyong@caas.cn (X.Y.Z.))

[Correction added on 18 April 2025, after first online publication: Abbreviated the author names in the author byline is updated in this version.]

Keywords: wheat, *Wox* gene, *TaWUS-like-5D*, TKW, grain development, yield.

Summary

Plant-specific *WUSCHEL-related homeobox* (*Wox*) transcription factors (TFs) are crucial for plant growth and development. However, the molecular mechanism of *Wox*-mediated regulation of thousand kernel weight (TKW) in crops remains elusive. In this research, we identified a major TKW-associated quantitative trait locus (QTL) on wheat chromosome 5DS by performing a genome-wide association study (GWAS) of a Chinese wheat mini-core collection (MCC) in four environments combined by bulked segregant analysis (BSA) and bulked segregant RNA-sequencing (BSR-seq) of wheat grains exhibiting a wide range of TKWs. The candidate *TaWUS-like-5D* was highly expressed in developing grains and was found to strongly negative influence grain TKW and wheat yield. Meanwhile, the RNAi lines, CRISPR/Cas9-edited single and double knockout mutants (AABB*dd* and AA*bbdd*), as well as the stop-gained *aa*BB Kronos mutants, exhibited a significant increase in grain size and TKW ($P < 0.05$ or $P < 0.01$) and a 10.0% increase in yield ($P < 0.01$). Further analyses indicated that *TaWUS-like-5D* regulates TKW by inhibiting the transcription of sucrose, hormone and trehalose metabolism-related genes, subsequently sharply decreasing starch synthesis in wheat grains. The results of this study provide a fundamental molecular basis for further elucidating the mechanism of *Wox*-mediated regulation of grain development in crops.

Introduction

Wheat (*Triticum aestivum* L.) is a globally important crop which is critical to ensuring food security in the world. Wheat production is expected to face serious challenges due to a combination of climate change and a projected doubling of the world population by 2050 (Godfray *et al*., 2010). Therefore, improving grain yield has become an urgent demand for wheat breeding. Thousand kernel weight (TKW) is one of the primary contributors to wheat grain yield and is determined by both grain size and plumpness (filling degree) (Gegas *et al*., 2010). In which, grain size is mainly composed by grain length (GL), grain width (GW), grain thickness (GT) and the GL/GW ratio (Gegas *et al*., 2010). Although genes regulating grain size and filling play vital roles in determining yield improvement in wheat, only approximately 20 TKW-related genes have been cloned in wheat to date (Jia *et al*., 2021; Liu *et al*., 2023; Yan *et al*., 2019). Thus, the molecular mechanism underlying yield-trait regulation in wheat remains largely unknown.

The plant-specific *WUSCHEL-related homeobox* (*Wox*) gene family encodes homeobox (HB)-containing transcription factors (TFs). HB-containing TFs are characterized by the presence of a 60–66 amino acid (aa) homeodomain (HD) (containing 12 conserved RQLYIVWFNRRK) with a helix–loop–helix–turn–helix structure (Gehring *et al*., 1990; Laughon, 1991), specifically for DNA sequence recognition and binding. Some Wox proteins also contain a distinct WUSCHEL (WUS)-box motif located at the carboxy-terminal end of the HD (Graaff *et al*., 2009), which is essential for the regulatory function of the Wox protein (Haecker *et al*., 2004; Skylar *et al*., 2010). WUS TFs play important roles in plant growth and development, including maintenance of meristematic stem cells in the shoot apical meristem (SAM) and root apical meristem (RAM), embryonic patterning, lateral organ development, floral induction, seed formation and regeneration of isolated tissues and organs (Hao *et al*., 2019; Jha *et al*., 2020; Leibfried *et al*., 2005). In *Arabidopsis*, 15 *Wox* (*AtWox*) gene family members have been identified, including the founding member *WUS* as well as *WOX1–WOX14*. According to phylogenetic analysis of HB domain-containing proteins in diverse plants, *Wox* family genes can be classified into three clades: the modern WUS clade (*WUS* and *WOX1–7*), the intermediate clade (*WOX8, 9, 11* and *12*) and the ancient clade (*WOX10, 13* and *14*) (Graaff *et al*., 2009). The various *AtWox* members have been functionally characterized (Haecker *et al*., 2004; Mayer *et al*., 1998; Zhang *et al*., 2010), and the majority of them have been found to perform meristem-related functions. For example, *AtWUS* is specifically required for the maintenance of shoot central meristem identity and floral meristem structural and functional integrity (Haecker *et al*., 2004; Laux *et al*., 1996; Mayer *et al*., 1998). *AtWOX5* performs a similar function in the RAM and is specifically expressed in the cells of quiescent centre (QC) (Gonzali *et al*., 2005; Sarkar *et al*., 2007). To date, at least 13 and 14 *Wox* genes have been, respectively, identified in rice (*Oryza sativa* L.) (Zhang *et al*., 2010) and wheat (Li *et al*., 2020).

Additional few *WUS* members have been identified in other dicotyledonous and monocotyledonous plants, including tomato (*Solanum lycopersicum*), melon (*Cucumis melo*), spruce (*Picea asperata*) and maize (*Zea mays* L.) (Graaff *et al*., 2009; Jha *et al*., 2020; Tang *et al*., 2023). However, aside from those in *A. thaliana*, only a few *Wox* members have been comprehensively studied, particularly those involved in the regulation of yield-related traits in gramineous crops. In rice, *OsWOX6* and *OsWOX11* are expressed asymmetrically in response to auxin connecting rice gravitropism response and were found control of rice tiller angle (Zhang *et al*., 2018). *DWARF TILLER1* (*DWT1*), a Wox TF homologous to *AtWOX8* and *AtWOX9*, is highly expressed in young rice panicles and was found to control main stem uniformity and tiller development (Wang *et al*., 2014a). *OsWOX3A* (*OsNS*), a rice *narrow leaf 2* and *narrow leaf 3* ortholog of *NARROW SHEATH1* (*NS1*) and *NS2* in maize and *PRESSED FLOWER* in *A. thaliana*, is involved in spikelet and tiller development (Cho *et al*., 2013). It is possible that these *Wox* genes may regulate grain yield by affecting plant architecture. However, because no *Wox* genes have been conclusively linked to TKW, the molecular mechanism underlying yield-trait control is still unclear.

In mature wheat grains, starch accounts for between 65% and 85% of the grain dry weight (Housley *et al*., 1981; Hurkman *et al*., 2003). Sucrose is the substrate for starch synthesis. Therefore, sucrose metabolism-related genes are key determinants of TKW and wheat grain yield (Figueroa and Lunn, 2016; Hou *et al*., 2014). As the primary photosynthetic end product, sucrose moves from sources to sinks through the phloem. Once unloaded by sucrose transporters (SUT and SWEET) in sink tissues, sucrose is first enzymatically cleaved into hexose and its derivatives in the cytoplasm and then transported into plastids by transporter proteins, where it is utilized as the substrate or energy for starch synthesis (Halford and Paul, 2003). Sucrose synthase (SUS/Susy, EC 2.4.1.13) catalyses the reversible cleavage of sucrose into fructose and either uridine diphosphate glucose (UDP-G) or adenosine diphosphate glucose (ADP-G) and is a key regulator of photosynthetic assimilate allocation to sucrose and starch (Stein and Granot, 2019). In gramineous crops, sucrose transport, unloading and metabolism are key determinants of grain filling and yield. However, the molecular mechanism regulating sucrose unloading and metabolism in wheat grains remains largely unknown.

In this study, we identified the TKW-related gene *TaWUS-like-5D* (*Triticum aestivum WUSCHEL-related homeobox-like 5D*) on chromosome 5DS through a genome-wide association study (GWAS) of a Chinese 262 mini-core collection (MCC) combined with bulked segregant analysis (BSA) and bulked segregant RNA-sequencing (BSR-seq) of wheat grains exhibiting a wide range of TKWs. *TaWUS-like-5D* was found to be a member of the *WUS* clade of the *Wox* family. Overexpression (OE) of *TaWUS-like-5D* in wheat significantly reduced TKW by 3.4 g ($P < 0.01$ and $P < 0.05$) and grain yield by 48.3% ($P < 0.01$), while these traits were increased in RNA interference (RNAi) lines by 2.9 g ($P < 0.01$ and $P < 0.05$) and 10.0% ($P < 0.01$). *TaWUS-like-5D* appears to regulate TKW by transcriptionally inhibiting genes related to sucrose lysis and utilization, as well as trehalose-6-phosphate (T6P) synthesis-related genes, thereby sharply reducing starch synthesis in wheat grains. The results of this study improve our understanding of the functions of *Wox* family members in regulating plant growth and development and provide a molecular basis for elucidating the mechanism of *Wox*-mediated regulation of grain development and yield.

Results

Mapping of TKW-associated gene *TaWUS-like-5D* by BSA combined with BSR-seq

A major quantitative trait locus (QTL) significantly associated with TKW was detected on chromosome 5DS based on a GWAS of a Chinese wheat MCC across four environments (Ge *et al*., 2012). We further narrowed this QTL down to a genetic distance spanning 2.94 cM using a TKW-related $F_{2:5}$ breeding population grown in four environments (Wang *et al*., 2015). The QTL is flanked by two simple sequence repeat (SSR) markers: *cfd78* and *cfd67*. To identify the candidate gene at this locus, a F_2 bi-parental segregation population exhibiting a wide range of TKWs was developed (Figure 1a,b) by crossing Chinese cultivar 'Zhongyou9507' with the Chinese 'Hongjinmai' landrace, with an average TKW difference of 36.32 g for the two bulks (Liu *et al*., 2023). Subsequently, BSA was used to fine-map the candidate gene on chromosome 5DS. On average, the BSA average sequencing depth for the two parents was 10.23-fold and for the two bulks was 26.88-fold. The clean reads produced 99.58%–99.74% coverage of the wheat reference genome (Table S1). In total, 38 678 601 single nucleotide polymorphisms (SNPs) and 3 413 246 insertions and deletions (InDels) were generated between the two bulks (CH and CL). According to SNP-index association analysis, the TKW-associated candidate gene was located in a 0.37-Mb genomic interval (108.08–108.45 Mb) on chromosome 5DS, with the average ΔSNP-index value line surpassing the 99% confidence interval thresholds (Figure 1c). According to gene annotation, the interval only contains five high-confidence genes. Among these, candidate genes *TraesCS5D03G0230700* and *TraesCS5D03G0230900* were previously uncharacterized in wheat and, respectively, encode a DNA-directed DNA polymerase and a complex 1 protein belonging to the LYR family in *A. thaliana*. Candidate genes *TraesCS5D03G0230800*, *TraesCS5D03G0231100* and *TraesCS5D03G0231500*, respectively, encode a *WUSCHEL-related homeobox 5-like* TF in rice and wheat, a boron transporter 1-like protein in wheat and *A. thaliana* and an NPG1 protein in wheat and *A. thaliana*. All five genes exhibited base differences between the two parents, but only *TraesCS5D03G0230800* exhibited SNP/haplotype (*Hap*) differences in Landraces and modern cultivars among the Chinese 262 MCC (Figure S1). According to association analysis, these variations were significantly associated with TKW, however, the others are not.

According to BSR-seq on wheat grains at 10-day post-anthesis (DPA), *TraesCS5D03G0230800* was the only gene found to exhibit high and differential expression between the parental pool and the bulk pool (Figure 1d). Because this candidate gene belongs to the *WUS* clade of the *Wox* family, it was designated as *TaWUS-like-5D*. Surprisingly, we identified the SSR marker *cfd78*, which has been reported to strongly affect TKW and to be located on chromosome 5DS (Wang *et al*., 2015), located in the promoter region (2.1 kb) of *TaWUS-like-5D*. Further *Hap* evolution analysis indicated that this gene has undergone moderate breeding selection (Figure 1e), forming four large germplasm *Haps* (*gHaps*) in modern cultivars. Therefore, *TaWUS-like-5D* was identified as the candidate gene associated with TKW

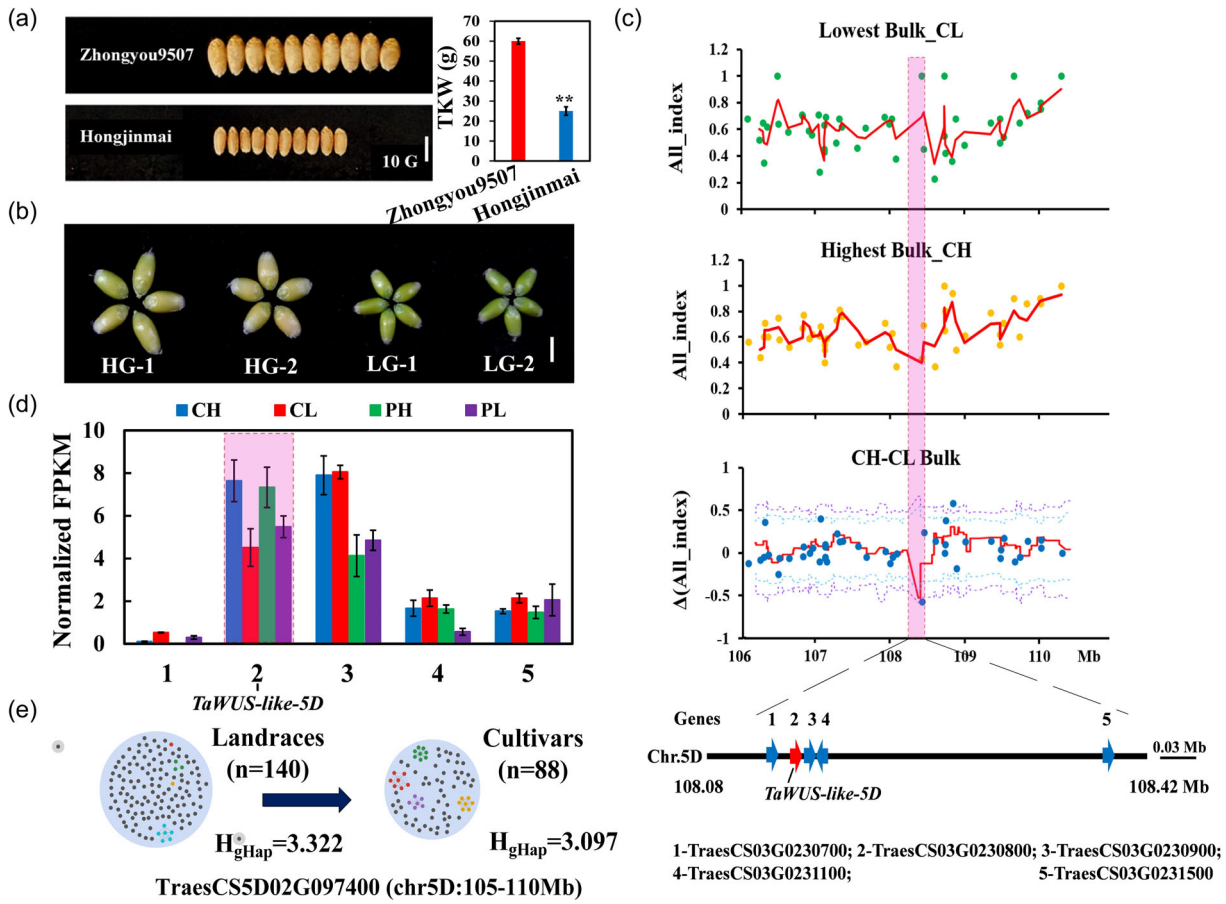

Figure 1 Cloning and identification of TKW-associated gene *TaWUS-like-5D*. (a) Mature grains and TKWs of the two parents used in BSA-seq mapping. 'Zhongyou9507', maternal parent (MTKW = 60.2 g); 'Hongjinmai', paternal parent (MTKW = 24.8 g). Bars = 1 cm. $^{**}P < 0.01$. (b) Grain phenotypes of the hybrid F_2 generation with either high TKW (HG) or low TKW (LG). (c) BSA-seq-derived genome-wide association signals for TKW are shown in the 106–115 Mb region on chromosome 5DS. The *x*-axis represents wheat chromosomes. The *y*-axis represents the SNP and InDel (All)-index and the ΔSNP (All)-index values. Red dashed lines represent the average SNP/ΔSNP-index values obtained using sliding window analysis with a 1-Mb window and 10-kb increments along the CS wheat reference genome. Green, yellow and blue dots indicate values in the CH, CL and subtraction pools, respectively. Pink vertical shading indicates the peak SNP position. Blue and purple horizontal dashed lines indicate the genome-wide significance thresholds at the 95% and 99% confidence intervals, respectively. Candidate regions are defined as regions where the ΔSNP-index values are greater than the threshold. (d) Expression profiles of the five candidate genes. DEGs were drawn from two parental pools (PL, PH) and two hybrid progeny bulks (CL, CH). Pink shading indicates the candidate gene *TaWUS-like-5D*. The expression level of each gene was normalized as FPKM for comparison. $N = 3$; bars = STDEV. (e) Haplotype breeding evolution analysis for *TaWUS-like-5D*. Each dot denotes a single accession. Linked dots denote *gHaps* (germplasm-type haplotypes in hexaploid wheat), and circles denote *aHaps* (ancestor-type haplotypes in wild Emmer). Different colours denote different haplotypes. H, haplotype Shannon diversity index. A Hutcheson t-test was used to determine statistically significant differences. $^{*}P < 0.05$; $^{**}P < 0.01$.

on chromosome 5DS and was subjected to further confirmation through transgenic experiments.

TaWUS-like-5D is a *WUSCHEL*-related homeobox-containing TF preferentially expressed in wheat grains

Protein aa sequence alignment of *TaWUS-like-5D* in the wheat database (http://202.194.139.32/) revealed that *TaWUS-like-5D* homoeologs were located on the short arms of chromosomes 5A and 5B. All three homoeologs consisted of two exons and one intron (Figure 2a). The lengths of the *TaWUS-like-5A*, *TaWUS-like-5B* and *TaWUS-like-5D* coding regions were 957, 966 and 969 bp, encoding 318, 321 and 322 aa, respectively. The TaWUS-like-5D protein shared high similarity with the TaWUS-like-5A (92.59%) and TaWUS-like-5B (91.36%) proteins, especially in the conserved homeobox domain (99.39%) and WUS box domain (100%) (Figure 2b), suggesting their functions may be conserved and redundant. The phylogenetic tree constructed using the WOX proteins of diverse plant species segregated the *TaWox* family as a separate evolutionary branch from other cereals (Figure 2e), suggesting that *TaWUS-like* genes may play specific roles in wheat.

Quantitative real-time PCR (qRT-PCR) revealed that *TaWUS-like-5D* is preferentially expressed in young spikes ($P < 0.05$) and developing grains ($P < 0.01$), with the highest expression level observed at 10 DPA (Figure 2c). Moreover, *TaWUS-like-5D* exhibited significantly lower expression in high TKW varieties than in low TKW varieties at the filling stage (5–10 DPA) ($P < 0.01$) (Figure 2c), suggesting that *TaWUS-like-5D* may be a negative regulator of grain filling. These results were validated by

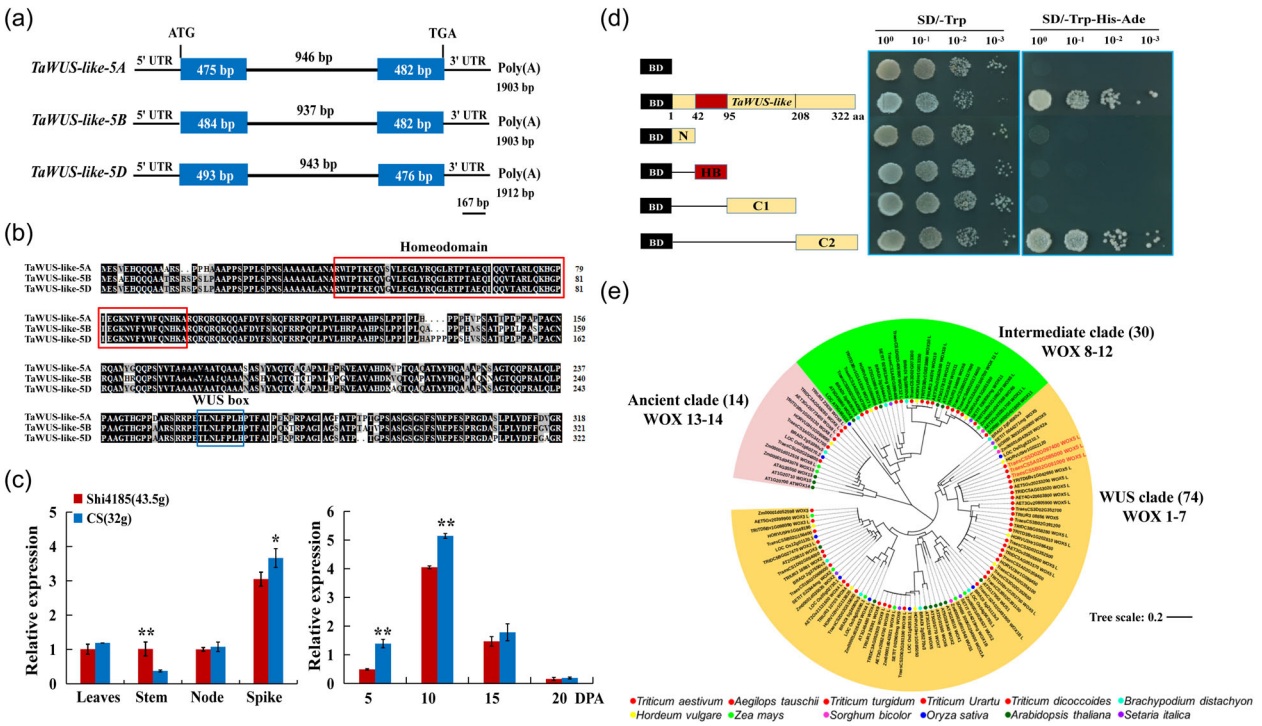

Figure 2 Expression and transcriptional activation characteristics of *TaWUS-like-5D*. (a) Genomic structures of three homoeologs of *TaWUS-likes*. Boxes correspond to exons. Dashes between the exons correspond to introns. Numbers correspond to the base number. 5′ UTR and 3′ UTR denote the untranslated upstream and downstream regions of the mRNA, respectively. (b) Predicted amino acid sequence comparison of the three homoeologs of TaWUS-likes. Red and blue boxes indicate the conserved DNA-binding homeobox domain and regulation/protein interaction domain WUS box (Swiss-Prot), respectively. (c) qRT-PCR expression profiles of *TaWUS-like-5D* in 'CS' (low TKW) and 'Shi4185' (high TKW) at different grain development stages and in different tissues. Leaves, roots, stems and nodes were sampled at the heading stages. Spikes were sampled at a length of 3–5 cm. DPA, days post-anthesis. *TaActin* was used as the internal control. Bars = standard error. $*P < 0.05$; $**P < 0.01$. (d) Transactivation activity assay of full-length and truncated TaWUS-like-5D proteins in yeast. Left, schematic diagram of TaWUS-like-5D protein. Right, analysis of transcriptional activation activity in 'Y2H Gold' yeast. Empty control vector BD was used as a negative control. 10^0–10^{-3} denote the dilution series. (e) Phylogenetic relationships among WUSCHEL-related homeobox (HB) superfamily proteins containing conserved HB domains in various plant species. Proteins containing sequences matching the HB domain were retrieved from the Ensemble Plants database. Pink, green and orange shading indicates different subfamily classifications of the *Wox* superfamily. Circled dots of different colours denote Wox proteins from different plant species. The neighbour-joining phylogenetic tree was constructed based on 1000 bootstrap replicates in MEGA 7.0.

the digital expression transcriptome data collected for the three homoeologs in Chinese spring (CS) wheat (Figure S2).

As expected for a TF, *TaWUS-like-5D* exhibited nuclear localization (Figure S3) and self-activation (Figure 2d). The transcriptional activation motif of *TaWUS-like-5D* was located at the C-terminus of the protein sequence (208–322 aa). These results were validated by a truncated aa segment activation experiment in yeast. These observations suggest that *TaWUS-like-5D* is a functional TF regulating wheat grain development.

TaWUS-like-5D negatively regulates wheat grain development and filling, resulting in lower TKW and yield

To study the biological function of *TaWUS-like-5D* in wheat, we generated *TaWUS-like-5D* OE and RNAi transgenic lines, CRISPR/Cas9-edited *CriTaWUS-likes* mutants in hexaploid wheat cultivar 'KN199' and *KTaWUS-like-5A/5B* mutants in tetraploid wheat 'Kronos'. Important agronomic traits, such as TKW, plant height (PH), grain number (GN), GL, GW, GT and tiller or spike number (TN/SN), were evaluated in these transgenic lines and mutants. OE of *TaWUS-like-5D* in wheat seriously impaired normal growth and grain development (Figure 3a). Compared with the wild-type (WT) 'KN199', the PH, TKW, GN and TN of OE plants were reduced by 14.0 cm, 3.4 g, 12.9 grains and 4.5 tillers, respectively ($P < 0.01$) (Figures 3b, S4a and S5, Table S2a). Notably, the tiller angle of the OE lines was increased by 23–42 degrees ($P < 0.01$) compared to tillers at the same positions in WT (Figure S6). The GL, GW and GT of the OE lines were decreased by 0.35 cm ($P < 0.01$), 0.38 cm ($P < 0.01$) and 0.35 cm ($P < 0.01$), respectively (Figure 3b).

The RNAi lines and mutants exhibited the opposite phenotypes. Compared to WT, the PH, TKW, GN and TN of the RNAi lines were increased by 1.2 cm, 2.9 g ($P < 0.01$), 2.5 grains and 1.0 tillers, respectively. The GL, GW and GT of the RNAi lines increased by 0.16 cm ($P < 0.05$), 0.11 cm ($P < 0.05$) and 0.1 cm ($P < 0.05$), respectively. However, the tiller angles of the RNAi lines were not significantly different than those of the WT. Compared to WT, the *CriTaWUS-likes* and *KTaWUS-likes* mutants exhibited a significant increase in TKW ($P < 0.05$, AABB*dd*, AA*bbdd*; $P < 0.01$, *KTaWUS-like-5A*), GL ($P < 0.01$,

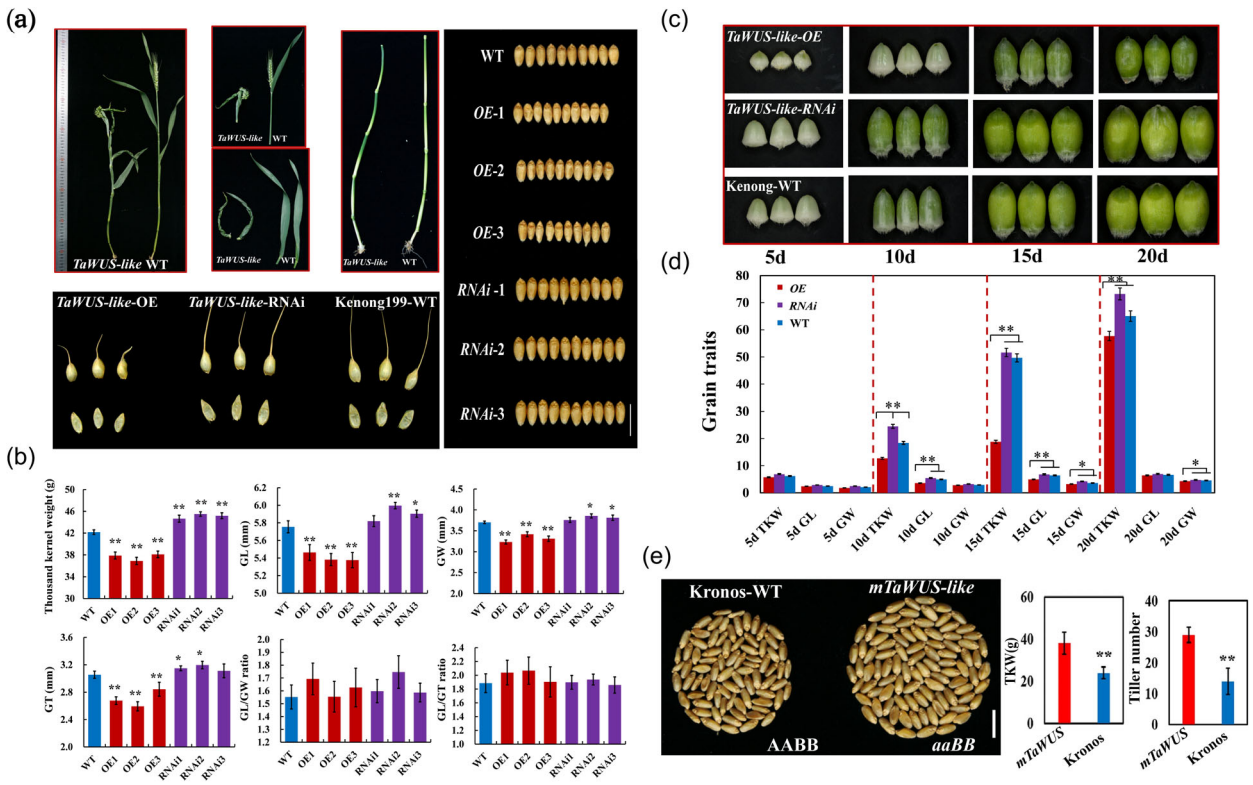

Figure 3 Mature grain phenotypes and agronomic traits of the *TaWUS-like-5D* OE and RNAi lines and *KTaWUS-likes* knockout mutants. (a) Whole-plant, mature grain, lemma and palea phenotypes of *TaWUS-like-5D* OE and RNAi lines and WT 'KN199' plants. The grains of different lines exhibited significant differences in width. $N = 10$ grains; Bars = 1 cm. (b) Grain traits of *TaWUS-like-5D* OE and RNAi lines and WT plants. TKW, thousand kernel weight; GL, grain length; GW, grain width; GT, grain thickness; GL/GW, ratio of GL to GW; GL/GT, ratio of GL to GT. $*P < 0.05$; $**P < 0.01$. (c) Developing grain phenotypes of *TaWUS-like-5D* OE and RNAi lines and WT plants. (d) Developing grain traits of *TaWUS-like-5D* OE and RNAi lines and WT plants. (e) Mature grain phenotypes and agronomic traits of *KTaWUS-like-5A* knockout mutants. Kronos denotes the WT AABB genome; *mTaWUS* denotes the mutated *aa*BB genome of *KTaWUS-like-5A* (stop-gained mutant) in tetraploid wheat kronos background.

aabbdd, AABB*dd*), GW ($P < 0.05$, AABB*dd*, AA*bbdd*), GT ($P < 0.01$, $P < 0.05$, AABB*dd*, AA*bbdd*), TN/SN ($P < 0.01$, *KTaWUS-like-5A*) and PH ($P < 0.05$, *KTaWUS-like-5A*; $P < 0.01$, $P < 0.05$, AABB*dd*, *aabbdd*) (Figures 3e, 4a–e, S7 and S8). Taken together, these results indicate that TKW and various grain traits are stable yield-related parameters affected by *TaWUS-like-5D*.

In the developing grains of the transgenic OE and RNAi lines, notable differences were detected in TKW ($P < 0.01$) and other grain traits ($P < 0.01/0.05$) as early as at 10 DPA (Figure 3c,d). Changes in the size of the lemma and palea of the transgenic lines further confirmed the role of *TaWUS-like-5D* in regulating grain TKW (Figure S9). Specifically, OE of *TaWUS-like-5D* resulted in shorter lemma and palea ($P < 0.01$) and narrower palea ($P < 0.05$) compared to the WT and RNAi lines. Yield per plant and grain yield under field conditions were estimated for the OE and RNAi lines using yield-related parameters (Figure S4b). The average yield of the OE lines decreased by 48.3% ($P < 0.01$) between 2016 and 2019, but increased by 10.0% in the RNAi lines ($P < 0.01$, 2016 only). These results further underscore the importance of *TaWUS-like-5D* in regulating grain TKW and wheat grain yield. In *A. thaliana*, OE of *TaWUS-like-5D* resulted in dwarfism, delayed bolting and flowering date, shorter pods, and lower yield (Figure S10). These effects are largely consistent with those observed in wheat, suggesting that *TaWUS-like-5D* might negatively regulate grain development and filling in wheat.

TaWUS-like-5D decreases amylose and amylopectin synthesis in wheat grain endosperm, resulting in lower starch content in grains

To verify the TKW-regulating function of *TaWUS-like-5D* in wheat, we evaluated the total starch, amylose and amylopectin contents, as well as the starch granule morphology, in the grain endosperm of the transgenic and mutant lines. Compared with the WT and RNAi lines, OE of *TaWUS-like-5D* resulted in significantly lower total starch, amylose and amylopectin contents in grain endosperm ($P < 0.01$) (Figure 5a). Compared to OE and WT, the RNAi lines exhibited only a decreased amylose/amylopectin ratio ($P < 0.05$). With the exception of the triple-knockout-mutant *aabbdd*, the *CriTaWUS-likes* mutants exhibited increased total starch (AABB*dd*, $P < 0.05$; AA*bbdd*, not statistically significant) and amylose (AABB*dd*, $P < 0.01$; AA*bbdd*, $P < 0.05$) contents compared to WT (Figure 5c). These results suggest that *TaWUS-like-5D* significantly decreases starch synthesis in grain endosperm, resulting in lower TKW in OE lines. However, we also found that knocking out more *TaWUS-like-5D/5B/5A* homologous genes did not result in radically enhanced starch content. On the contrary, the total starch, amylose and amylopectin contents all decreased significantly ($P < 0.01$) in *aabbdd* mutants, consistent with the decreased TKW (Figure 4e, not statistically significant). *aabbdd* mutants also exhibited significantly increased GL (Figure 4e, $P < 0.01$) and inadequate

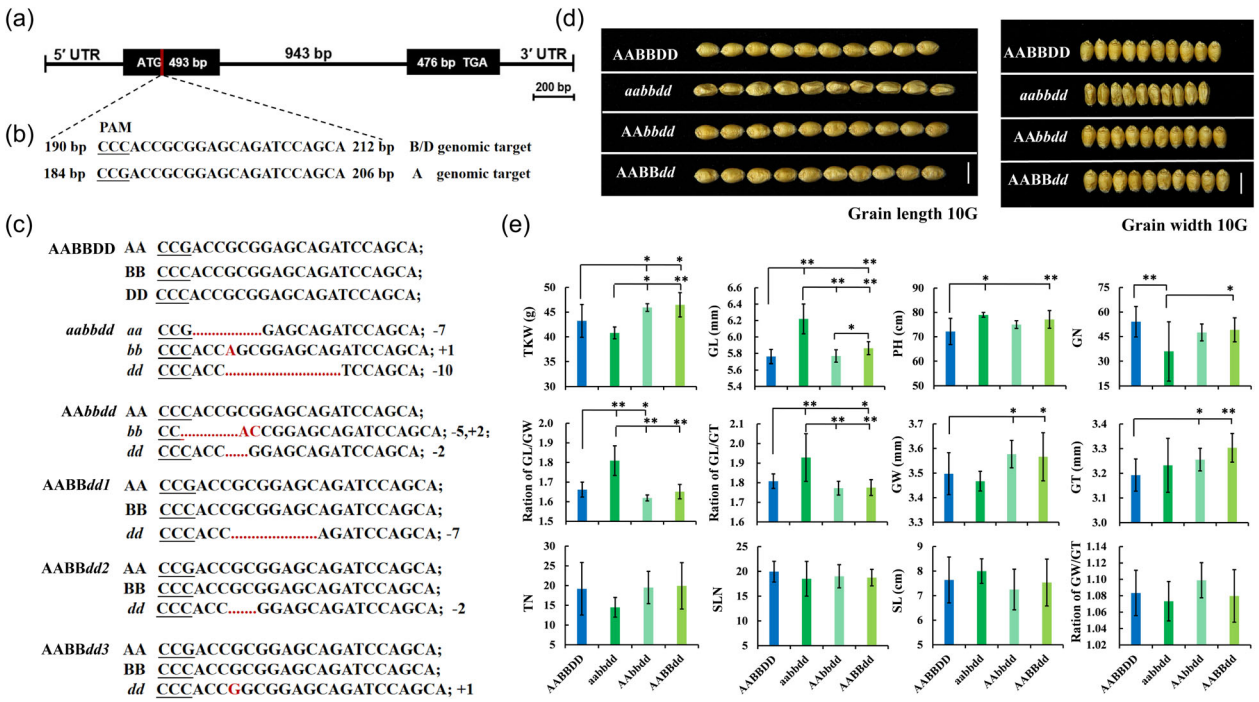

Figure 4 Mature grain phenotypes and agronomic traits of the *CriTaWUS-likes* knockdown mutants. (a) Schematic diagram of *CriTaWUS-likes* mutants generated using CRISPR/Cas9. Black boxes correspond to exons. Dashes between the exons correspond to introns. Numbers correspond to the base number. 5′ UTR and 3′ UTR denote the untranslated upstream and downstream regions of the mRNA, respectively. Red boxes within the gene model represent sgRNA target sites. (b) Sequences are shown underneath the underlined protospacer-adjacent motif (PAM). (c) Genotypes of the mutant lines. The base sequence shows the sgRNA target sites and the PAM is underlined. Capital letters (AA/BB/DD) and italic lowercase letters (*aa*/*bb*/*dd*) denote WT and mutant chromosomes, respectively. Red letters within the sequence indicate nucleotide insertions, and red dashed lines represent nucleotide deletions. Numbers with plus or minus correspond to the bases specifically inserted or deleted. (d) Grain traits of the *CriTaWUS-likes* mutants. The grains of different lines exhibited significant differences in length and width. $N = 10$ grains (G); Bars = 1 cm. (e) Agronomic traits of the *CriTaWUS-likes* mutants. TKW, thousand kernel weight; GL, grain length; GW, grain width; GT, grain thickness; GL/GW, ratio of GL to WK; GL/GT, ratio of GL to GT; PH, plant height; GN, grain number; TN, tiller number; SLN, spikelet number; SL, spike length. *$P < 0.05$; **$P < 0.01$.

grain filling (Figure 5e). Typically, a significant decrease of starch content in grains leads to a corresponding increase in protein levels. To check this 'seesaw' balance, protein levels in the transgenic lines were determined using near-infrared reflectance spectroscopy. The results indicated that for the OE ($P < 0.01$) and RNAi (not statistically significant with WT) transgenic lines, as well as the *aabbdd* mutant ($P < 0.01$), the expected 'seesaw' pattern was observed (Figure S11); however, for the AABB*dd* ($P < 0.05$) and AA*bbdd* (not statistically significant with WT) mutants, both showed an increase in both the starch and protein contents. These results suggested that *TaWUS-likes* regulate the conversion of sucrose to starch and the balance between starch and protein by a complex network. It appears that the expression levels and the balance among the three homologous genes are also necessary for the normal wheat grain development and particularly for adequate grain filling.

For the grain images, the OE lines exhibited a significant decrease in the total number of starch granules ($P < 0.01$), as well as fewer ($P < 0.05$) and smaller (granule diameter, $P < 0.01$) spherical A-type starch granules (Figure 5b). The average starch granule diameter decreased by 31.8% ($P < 0.01$) compared to WT (Figure 5b). Furthermore, approximately 10%–26% of A-type starch granules in OE grains exhibited sunken surfaces, and approximately 63% of the shrivelled OE grains exhibited large cavities in the endosperm (Figure 5d), indicative of inadequate filling in OE lines. In contrast, the WT starch granules were arranged regularly and packed densely, with no obvious cavities in the endosperm. The total number of distorted starch granules did not differ significantly between WT and RNAi lines. For the *CriTaWUS-likes* mutants, a significant increase in A-type granule diameter was observed in AABB*dd* mutants ($P < 0.01$, Figure 5e, f), and a significant decrease in both total granule number and A-type granule diameter was observed in *aabbdd* mutants ($P < 0.01$), compared with WT. However, no significant differences were observed between WT and AABB*dd* and AA*bbdd* mutants in the number of A-type granules or between WT and AA*bbdd* mutants in granule diameter. Interestingly, we observed larger and fuller A-type granules in AABB*dd* mutants, a greater number of B-type granules in AA*bbdd* mutants, and inadequate grain filling in *aabbdd* mutants (Figure 5e). These results were consistent with the TKW and starch content phenotypes of AABB*dd* and *aabbdd* mutants and suggest sub-function-differentiation among *TaWUS-likes* homologous genes in regulating sucrose conversion. Together, these results confirmed the importance of *TaWUS-like-5D* in regulating starch synthesis in wheat grains.

TaWUS-like-5D affects starch synthesis by regulating sugar signal T6P, sucrose lysis and utilization, and phytohormone level and balance

Transcriptomic sequencing of wheat grains was performed to elucidate the molecular mechanism of *TaWUS-like-5D*-mediated

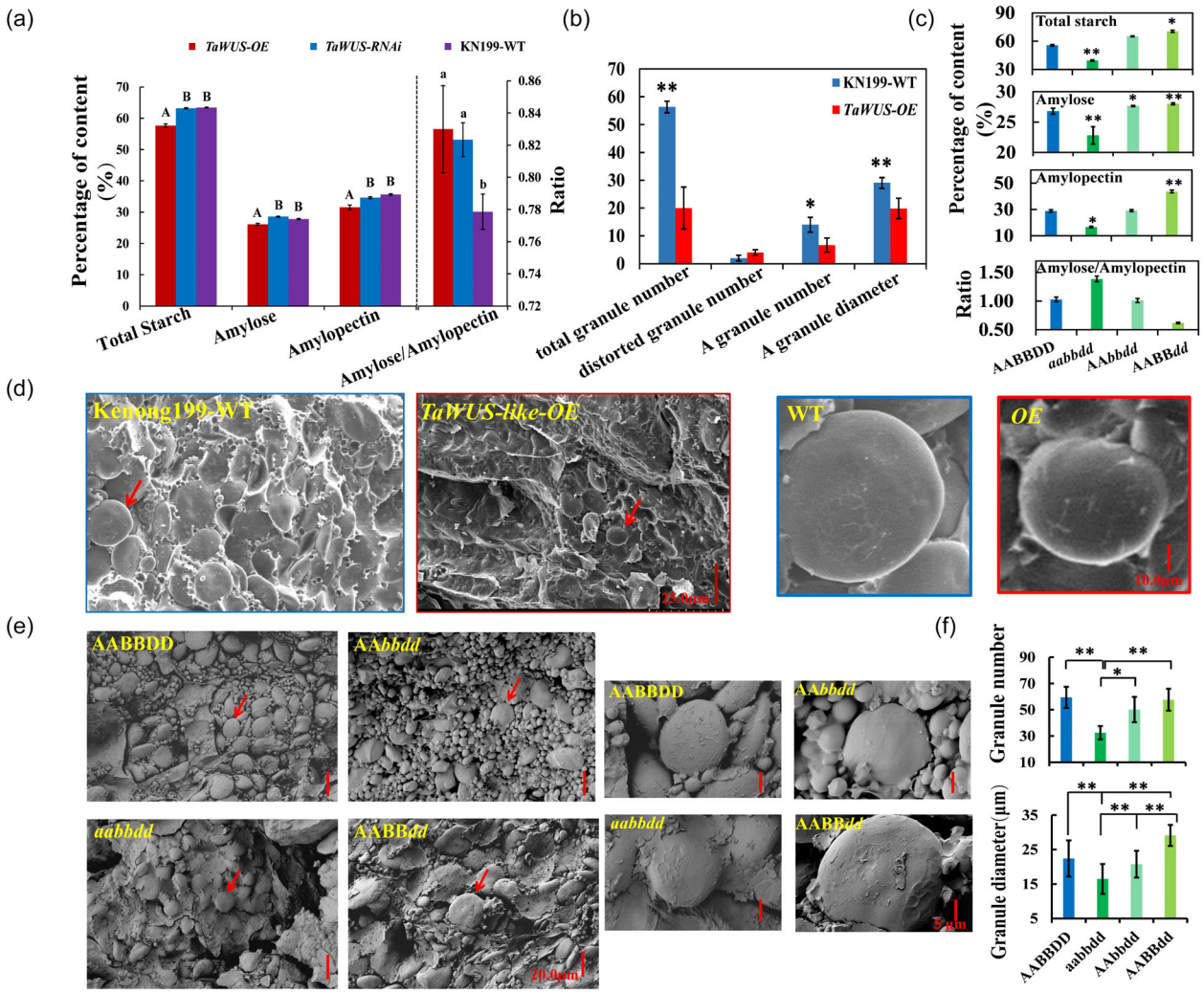

Figure 5 Starch contents and starch granule characteristics of *TaWUS-like-5D* OE lines and *CriTaWUS-likes* mutants. (a, c) The contents of total starch, amylose and amylopectin, as well as the ratio of amylose to amylopectin, in *TaWUS-like-5D* OE and RNAi lines (a), *CriTaWUS-likes* mutants (c) and WT plants (a, c). Lowercase letters and $*P < 0.05$; capital letters and $**P < 0.01$. In the pairwise comparison, non-significant differences are indicated when the letters are the same. (b, f) Number of granules and granule diameter in *TaWUS-likes* OE lines (b), *CriTaWUS-likes* mutants (f) and WT plants (b, f). $*P < 0.05$; $**P < 0.01$. $N = 3/4$; Bars = STDEV. (d, e) Scanning electron microscopy (SEM) images of starch granules extracted from the mature grains of *TaWUS-like* OE lines (d), *CriTaWUS-likes* mutants (e) and WT plants (d, e). Red arrows indicate selected enlarged granules of OE, *CriTaWUS-likes* mutants, and WT grains. $N = 3/4$. Bars = 25 μM (OE) or 10 μM (WT); Bars = 20 μM (*CriTaWUS-likes* mutants) or 5 μM (WT).

regulation of starch synthesis. In total, 84 356 differentially expressed genes (DEGs) were identified among the OE, RNAi and WT plants. Among these, 4517 and 1616 DEGs were specifically expressed in the OE and RNAi lines, respectively.

The majority of sucrose and starch metabolism- and regulation-related genes were significantly inhibited by *TaWUS-like-5D* in the developing grains (Figures 6a and S12–S14, Table S5). In grains at 10 DPA, the expression levels of several notable genes were all at least twofold lower in the OE lines than in the WT lines, including sucrose synthase (SUS) genes *SUS-2A/2B/2D/7B/7D/3B*; starch synthesis genes (SS) *SS-7A/7B/7D*; starch branching enzyme (SBE) gene *SBE-2A*; cell wall cellulose synthesis (CesA) and like (CeL) genes *CesA-1D/2A/3B/5B/5D/6A* and *CeL-3B*; T6P sugar signal synthesis genes *TPS-1A/5D/6B* and *TPS6-1A/3A/3B/3D*; and T6P phosphatase gene *TPP-6D* (Figure 6a). At 15 and 20 DPA, most still exhibited at least twofold lower expression (Figure S12), including *SUS-3B*, *SBE-2A*, *CesA-1D/3B/5D*, *CeL-3B*, *TPS-1A/6B*, *TPS6-1A/3B/3D* and *TPP-6D* at 15 DPA and *SUS-2A/2B/2D/7D*, *SBE-2A*, *CesA-1B/3D* and *TPP-6B/7D* at 20 DPA. These results suggest that T6P and sucrose metabolism-related genes were the primary downstream targets of *TaWUS-like-5D*, thereby affecting grain filling and TKW.

Moreover, several phytohormone synthesis- and signal transduction-related genes and TFs (Figures S13 and S14) were also significantly affected by *TaWUS-like-5D* in the developing grains of the OE lines. For example, at 10 DPA, the expression levels of cytokinin (CTK) synthesis gene *IPT-1D/5A/5D*, auxin response factor (ARF) gene *ARF-3B* and auxin-responsive TF gene *TCP-5B* were at least twofold lower in OE lines than in WT lines. Conversely, the expression levels of gibberellin (GA) and abscisic acid (ABA) synthesis-related genes such as *GA3ox-2A* and *NCED-5B*, as well as the *TaNAC019-A* TF (Gao *et al.*, 2021) were increased approximately 5.0-fold, 1.9-fold and 2.6-fold in OE grains compared to WT grains at 10 DPA. The expression changes

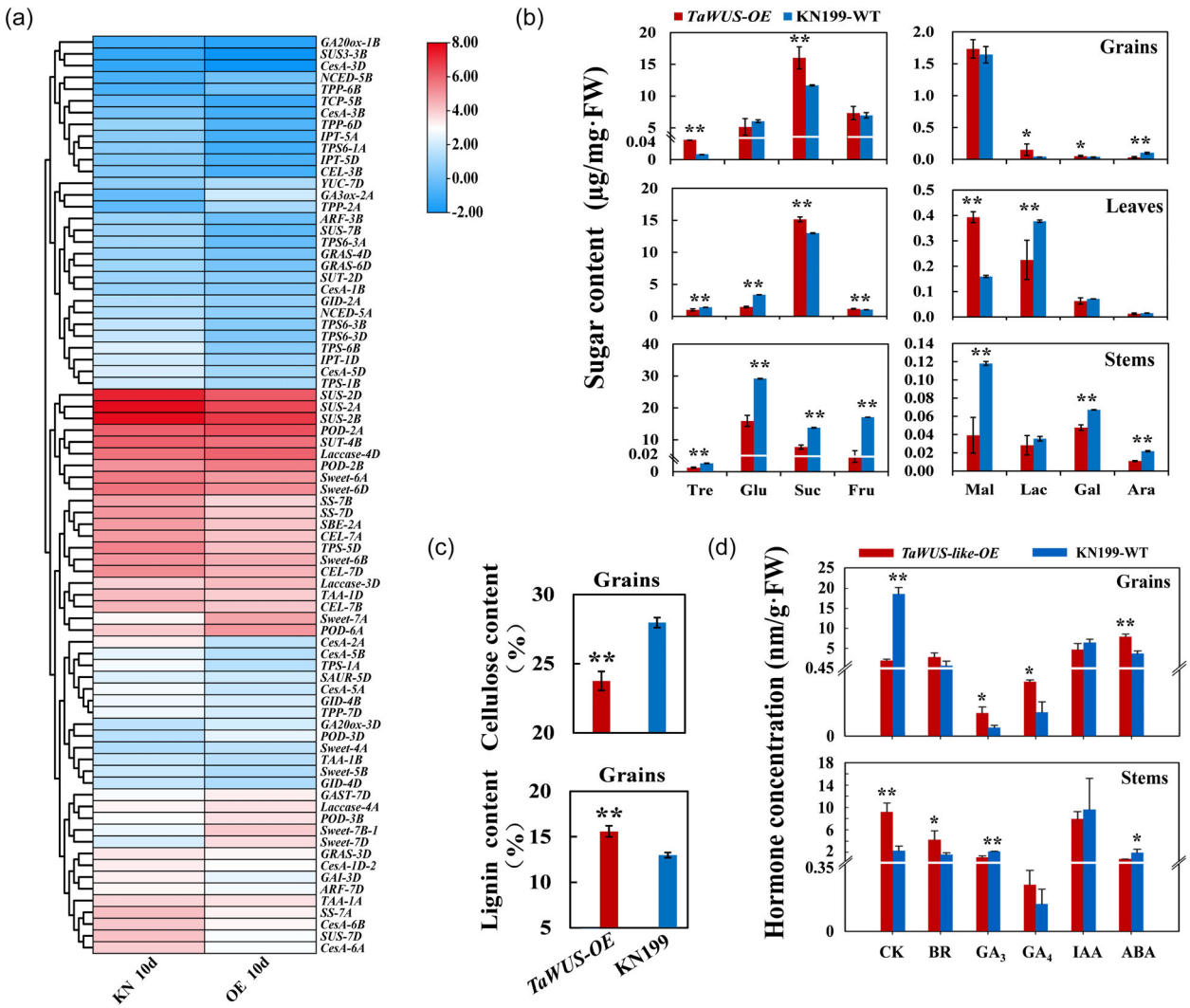

Figure 6 *TaWUS-like-5D*-regulated downstream gene identification, sugar content and phytohormone levels. (a) Cluster heatmap of downstream genes regulated by *TaWUS-like-5D* in 10 DPA grains of transgenic OE lines and WT plants. The averages of three experiments are shown. The $\log_2$ fold change scale is indicated on the right side of the heat map. Full gene names and IDs can be found in Table S6. (b) The contents of sucrose, trehalose and other sugars at 10 DPA in grains, fresh leaves and stems. Bars = STDEV. *$P < 0.05$; **$P < 0.01$. (c) The contents of cellulose and lignin at 10 DPA in the grains of *TaWUS-like-5D* OE lines and WT plants. (d) The contents of phytohormones in 10 DPA grains and stems. CK, cytokinin; BR, brassinolide; GA_3 and GA_4, gibberellin; IAA, auxin; ABA, abscisic acid. [Correction added on 19 March 2025, after first online publication: Figure 6 is updated in this version.]

of these genes help explain certain phenotype changes, including the decreased grain size, reduced starch content and the increased protein levels in the grains of the OE lines. This suggests that a variety of phytohormones and TFs are also involved in the regulation of starch synthesis in the grain endosperm, and consequently, influence grain size, filling and TKW.

We next evaluated the contents of the soluble carbohydrates and phytohormones in flag leaves, stems and grains to verify the effects of *TaWUS-like-5D* on endogenous sugar metabolism and phytohormone dynamics. At 10 DPA, the grains of OE lines contained significantly higher contents of sucrose, trehalose, lactose and total sugar compared to WT grains ($P < 0.01$ and $P < 0.05$; Figure 6b). However, compared to WT, OE leaves and stems contained significantly lower contents of glucose and trehalose ($P < 0.01$); OE stems contained significantly lower contents of sucrose, fructose, maltose and the other sugars ($P < 0.01$); and OE leaves contained a significantly higher contents of sucrose and maltose ($P < 0.01$), indicative of different sugar distribution and regulatory mechanisms in different wheat tissues, especially between the grains and stems. The contents of cellulose, lignin and phytohormones in OE grains were also evaluated (Figure 6c,d). At 10 DPA, OE grains contained significantly lower contents of cellulose ($P < 0.01$) and CTK ($P < 0.01$), and significantly higher contents of lignin ($P < 0.01$), GA ($P < 0.05$) and ABA ($P < 0.01$), than WT grains. Surprisedly, the GA_3, CTK and ABA concentrations in OE stems exhibited an opposite changing trend to those in grains, suggestive of these phytohormones may be involved in regulating sugar distributions. However, these results were consistent with the expression patterns of *CesA*, *POD*, and CTK-, GA- and ABA-synthesis genes in the developing OE grains (Figures 6a and S12). Therefore, these observations further confirmed the point that *TaWUS-like-5D* affects starch synthesis and grain filling mainly by regulating and balancing sugar and hormone levels.

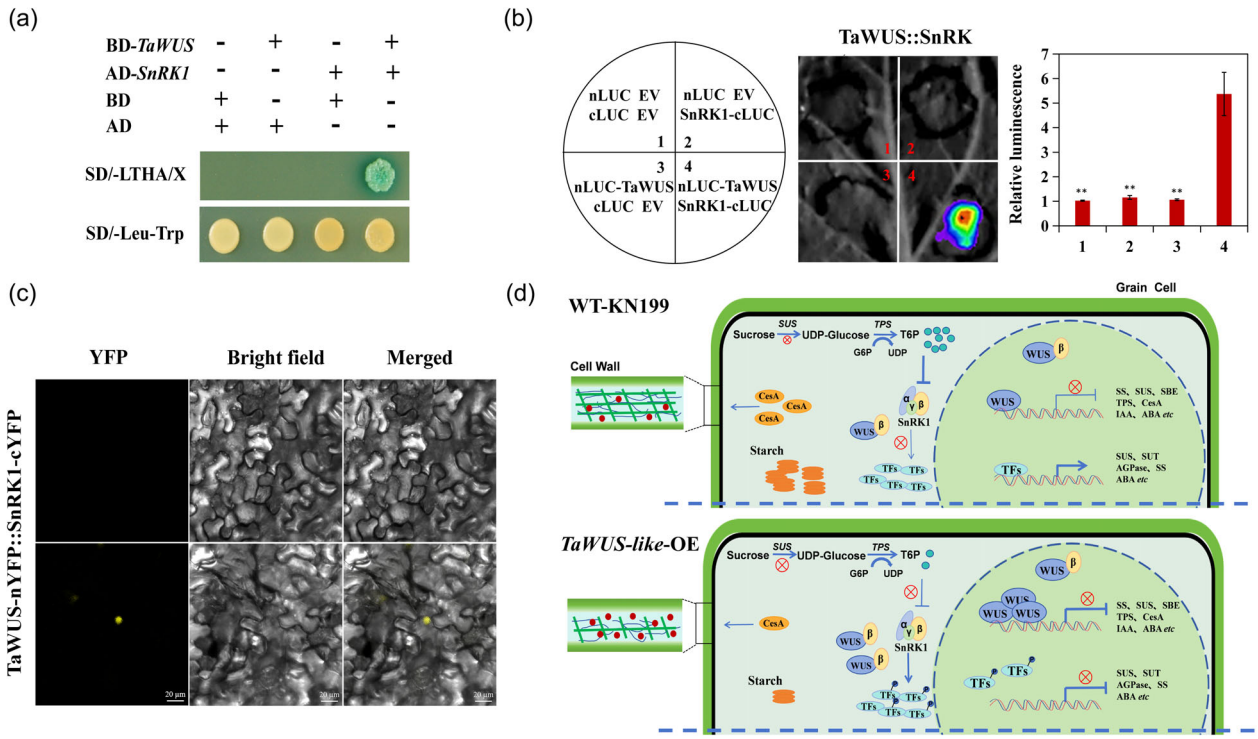

Figure 7 TaWUS-like-5D physically interacts with TaSnRK1-4B. (a) Y2H assay showing that TaWUS-like-5D interacts with TaSnRK1-4B in yeast cells. SD/-Leu-Trp and SD/-LTHA/X denote the synthetic dextrose bidruple (lacking Trp and Leu) and quadruple (lacking Leu, Trp, His and Ade) dropout media, respectively. X denotes the chromogenic β-galactosidase substrate X-gal. BD and AD denote the empty bait and prey vectors, respectively. (b) LCI assay illustrating the interaction between TaWUS-like-5D and TaSnRK1-4B in *N. benthamiana*. Luciferase signals were detected 48-h post-infiltration. Data represent the averages of five biological replicates ± STDEV ($N = 5$). $^{**}P < 0.01$. (c) BiFC assay confirming the physical interaction of TaWUS-like-5D with TaSnRK1-4B in *N. benthamiana*. YFP fluorescence was detected 48-h post-infiltration. The cYFP and nYFP-TaWUS-like-5D vectors were co-infiltrated into *N. benthamiana* leaves as a negative control. $N = 5$. Bars = 20 μm. (d) A proposed working model of the molecular modulation network underlying *TaWUS-like-5D*-mediated sugar metabolism and starch synthesis in wheat grains. TaWUS-like-5D protein inhibits the expression of *SUS*, *CesA*, *SS* and *TPS*; alters phytohormone levels; affects T6P-SnRK1 signalling pathway; and interacts with the β-subunit of SnRK1-4B. These mechanisms subsequently affect starch synthesis in wheat grains. SnRK1 was composed by α, β (yellow oval) and γ subunit. Blue lines with arrows illustrate the fate of sucrose (e.g. to cell wall, to starch and to T6P signalling pathway) in metabolic step and activation effect among genes. Blue lines with blue vertical lines and the red cross in circles including the thickness of the lines and sizes of the circles indicates the inhibitory effect and degree of T6P on SnRK1 activity in wheat grains (Martínez-Barajas *et al.*, 2011; Liu *et al.*, 2023) or among genes. The changes of the green lines and red dot in cell wall denote the content changes of the cellulose and lignin, respectively. Inhibitory effects of *TaWUS-like-5D* were supported by experimental validation of transcriptomic data, sugar content and phytohormone levels.

TaWUS-like-5D physically interacts with SnRK1-β1-4B in wheat grains

Protein interactions play an important joint or inactive role in the normal function of TFs. A yeast two-hybrid (Y2H) system was utilized to identify factors interacting with the TaWUS-like-5D TF. We found that the SNF1-related protein kinase regulatory subunit beta-1 protein SnRK1-β1-4B could interact with TaWUS-like-5D in yeast (Figure 7a). To verify the interaction, we performed a firefly luciferase dual-complementation reporter (LDR) assay and bimolecular fluorescence complementation (BiFC) assay in tobacco (*Nicotiana benthamiana*) cells. The co-infiltration of nLUC-TaWUS-5D and SnRK1-4B-cLUC resulted in a fivefold stronger luminescence interaction signal than the other three pairs of co-infiltration samples generated by the complemented luciferase (Figure 7b). Similarly, interaction signals were detected in the TaWUS-nYFP and TaSnRK1-cYFP co-expressed samples. However, no YFP fluorescence signals could be detected in the control samples (Figure 7c). These results provide strong evidence that TaWUS-like-5D physically interacts with SnRK1-β1-4B in wheat grains, and therefore, TaWUS-like-5D protein may be involved in regulating sugar and ABA interaction by affecting SnRK1 signalling pathway, and consequently, affect starch synthesis (Figure 7d).

Discussion

TKW is one of the major determinants of wheat grain yield. Therefore, identifying novel genes regulating grain size and filling is crucial for improving wheat yields. Here, we identified one major TKW-related gene *TaWUS-like-5D* on chromosome 5DS through a combination of GWAS, BSA and BSR-seq. According to protein sequence alignment and phylogenetic analysis, this gene was found to belong to the *WUS* clade of the *Wox* family and to be clustered in a cereal-specific evolutionary branch. Analysis of gene expression in various tissues and at different grain developmental stages suggested that *TaWUS-like-5D* plays a specific novel role in wheat. Specifically, *TaWUS-like-5D* acts as

a negative regulator of wheat grain yield by inhibiting sucrose lysis and utilization, as well as T6P synthesis, and modulating phytohormone balance (Figure 7d).

Although a growing body of research suggests that *WUSCHEL* family members regulate plant growth and development in various dicots and monocots, little is known regarding the function of *WUSCHEL* family members in regulating TKW in grain crops. Recently, Yoshida *et al*. (2023) identified a grass-specific homeobox-containing transcription factor *OsWOX9D* in rice by GWAS using a Japanese rice breeding population and found that *OsWOX9D* enhances grain width for better sake brewing, and however, the molecular mechanism underling grain size-regulation still remain elusive. To our knowledge, our study is the first report of the role of *WUSCHEL* family members in regulating grain yield by affecting sucrose and hormones metabolism. Interestingly, we found that *TaWUS-like-5D* did not lose its residual meristem function when ectopically overexpressed in wheat. In fact, TN and PH were significantly reduced in OE lines compared to WT plants, suggesting that *WUSCHEL* family genes exhibit conserved functions in monocots and dicots. Therefore, *TaWUS-like-5D* and other *WUSCHEL* family members have the potential to regulate yield-related traits in crop plants.

However, to date, only approximately 20 TKW-related genes have been cloned in wheat. Although certain molecular mechanisms underlying grain size and filling appear to be conserved between monocots and dicots, such as the orthologous genes found in *A. thaliana*, rice, maize and wheat. For examples, *TaGW2*, the orthologous gene of *OsGW2* in rice, has also been found to participate in the ubiquitination-mediated proteasomal degradation pathway and ultimately to decrease grain width (Su *et al*., 2011); *TaGW8* (Yan *et al*., 2019) and *TaGASR7* (Zhang *et al*., 2015), SPL and GRAS family TFs which also regulate grain size and yield in rice (Li *et al*., 2018; Zuo and Li, 2014); the molecular regulatory mechanisms underlying TKW-trait regulation are still largely unknown.

Here, we found that *TaWUS-like-5D* regulates TKW by modulating sucrose metabolism and phytohormone signalling, representing a fairly novel or an important but presently unknown molecular regulatory mechanism. At the very least, sucrose metabolism and signalling play extremely important roles in crop grain development than the ones in *Arabidopsis* and other dicots plants, since in contrast to other tissues and plants, the starch content in wheat grains often exceeds 65% of dry weight. Our results showed that at 10 DPA the OE grains contained 37.9% more sucrose ($P < 0.01$) than WT grains. At the same periods and tissues, the transcript levels of *SUS, SS, CesA* and *TPS* were down-regulated at least 2.0-fold in OE lines compared to WT plants. At the matured grains, the contents of total starch, amylose, amylopectin and cellulose were all significantly lower in OE than in WT grains. Taken together, these results showed clearly that a special potential role of *TaWUS-like-5D* regulating sucrose metabolism by affecting the activity of SUS, ultimately *TaWUS-like-5D* decreased the conversion of sucrose to starch, and the further utilization of sucrose to cellulose and T6P synthesis.

Notably, we also observed that the phytohormones content of the grains also changed significantly. Historically, it was thought that phytohormones alone were responsible for the regulation of seed development (Gao *et al*., 2023). For example, *TaCKX2A_2*, *TaCKX4A_2*, *TaCKX5A_3* and *TaCKX9A_2* (Shoaib *et al*., 2020) reduce CTK levels, while *TaGASR7* (Dong *et al*., 2014) is responsive to GA. These genes were reported to be associated with higher filling rates, and greater grain size and weight. OE of the ABA receptor *TaPYL1-1B* results in larger grains and higher grain yields (Mao *et al*., 2022). Here, we found that OE of *TaWUS-like-5D* altered the transcription of *IPT*, *GA3ox, NCED* and *SUS*, all important yield-related factors. These results suggest that hormone levels and balance, as well as hormone–sucrose interactions, together regulate grain weight. However, the precise regulatory mechanism underlying grain development in wheat and other grain crops remains elusive. Therefore, we suggest that the TaWUS-like-5D-mediated inhibition of *SUS* gene expression requires further experimental validation.

SUS belongs to the glycosyltransferase-4 subfamily of the multi-gene glycosyltransferase family and is considered the most important sucrose cleavage enzyme influencing plant growth, starch and cellulose synthesis, and anaerobic stress tolerance (Stein and Granot, 2019). In developing wheat and barley grains, peak *SUS* gene expression overlaps well with the expression of starch synthesis genes (Chevalier and Lingle, 1983; Kumar and Singh, 1980). Numerous research has revealed that the majority of *SUS* genes are expressed mainly in developing seeds and fruits (Fallahi *et al*., 2008; Xu *et al*., 2012). In addition, changes in *SUS* gene expression or SUS enzyme activity can significantly alter seed size, starch content and endosperm development. For example, inhibition of *SUS* transcription in maize (Chourey *et al*., 1998) and cotton (Ruan *et al*., 2003) results in small, shrunken seeds and lower seed weight. Meanwhile, increased SUS enzyme activity is positively correlated with dry matter accumulation in rice grains, tomato fruits and potato tubers (Kato, 1995; Sun *et al*., 1992; Zrenner *et al*., 1995). In maize kernels, tomato fruits and carrot roots, reduced SUS enzyme activity resulted in a 62% (Chourey and Nelson, 1976), 34%–63% (Zrenner *et al*., 1995) and 26% (Tang and Sturm, 1999) decrease in starch content, respectively. These results suggest that *SUS* genes alter sink strength by regulating starch synthesis or seed development (Stein and Granot, 2019). Similar results were obtained in this study. Specifically, OE of *TaWUS-like-5D* resulted in decreased TKW and total starch content, inadequate grain filling, and increased sucrose and protein accumulation in wheat grains. The AABB*dd CriTaWUS-like-5D* single mutants exhibited the opposite phenotype except protein content, supporting the observation that *TaWUS-like-5D* inhibits *SUS* expression and that *SUS* enhances starch synthesis and sink strength in wheat grains. To date, six *SUS* genes have been identified in *A. thaliana* (Baud *et al*., 2004), as well as six in rice (Hirose *et al*., 2008) and three in maize (Carlson *et al*., 2002). However, only two *SUS* genes have been identified in wheat (Maraña *et al*., 1988). Association analyses have revealed that *TaSus1* and *TaSus2* are associated with increased TKW (Hou *et al*., 2014; Jiang *et al*., 2011). Our results confirm the importance of *TaSUS1/2* and their regulating factor TaWUS-like-5D in determining the sink strength of wheat grains. However, the regulatory mechanism of *SUS* gene expression in wheat grains is still largely unknown. SUS enzyme activity has been suggested as an indicator of high grain yield in rice breeding (Counce and Gravois, 2006). The same concept could be applied to wheat breeding. We suggest that wheat germplasm with increased grain yield could be created by engineering this negative regulator of sucrose and starch synthesis using CRISPR-Cas9 gene editing. In current study, we highlighted the potential breeding by knockout of the *TaWUS-like-5D* for creating the new wheat germplasms with enhanced both starch and protein levels in grain endosperm.

Recently, Liu *et al*. (2023) reported that the trehalose pathway component *TaTPP-7A* controls grain size and weight by regulating sucrose lysis, flux and utilization in the grain

endosperm via the T6P-SnRK1 pathway. Their results confirmed the T6P signalling pathway as the central mechanism regulating sucrose allocation and source-sink interactions in wheat grains. In this study, we found that *TaWUS-like-5D* significantly inhibited the transcription of *TPS*, a key enzyme responsible for the synthesis of T6P. Therefore, *TaWUS-like-5D* may play an important role in determining the enhancement of TKW and wheat yield by functioning as a negative regulator of the T6P signalling pathway. In *A. thaliana* and wheat, T6P responds to sucrose availability and thereby regulates carbohydrate allocation and utilization (Lunn *et al*., 2006; Martínez-Barajas *et al*., 2011; Nunes *et al*., 2013; Wingler *et al*., 2012). The catalytic activity of sucrose nonfermenting-1-related protein kinase 1 (SnRK1) is inhibited by T6P (Martínez-Barajas *et al*., 2011). The heterotrimeric complex SnRK1 is orthologous to the evolutionarily conserved SNF1/AMPK serine–threonine kinase in yeast and animals and contains one catalytic α-subunit and two regulatory β- and γ-subunits (Baena-González *et al*., 2007). Research suggests that SnRK1 is most likely involved in the starvation-responsive adjustment of metabolism and growth and therefore functions as a central regulator of metabolic homeostasis in plants (Broeckx *et al*., 2016; O'Hara *et al*., 2013).

According to the Y2H, LCI and BiFC assays, the TaWUS-like-5D protein physically interacts with the β- subunit of SnRK1. In addition, OE of *TaWUS-like-5D* significantly increased the transcription of *NCED*, a rate-limiting ABA-synthesis enzyme, as well as the ABA concentration of wheat grains. These results suggest that SnRK1 kinase activity may be affected by interaction with TaWUS-like-5D, and therefore, TaWUS-like-5D may regulate ABA signal transduction. ABA signal transduction is activated by SnRK1 and SnRK2, with the latter activated in the presence of ABA and by the breakdown of SnRK1. Liu *et al*. (2023) reported that reduced levels of T6P in wheat grains result in the activation of SnRK1 kinase activity and ABA signalling. Therefore, the T6P-SnRK1-ABA module plays an important role in the regulation of wheat grain filling. Our results confirm this concept, as T6P and SnRK1 were found to be the main two regulatory targets of *TaWUS-like-5D*, although the mechanism remains elusive. One early study found that silencing the *PKIN1* gene, which encodes an isoform of SnRK1α in potato tubers, down-regulated the expression of *SUS4* and reduced SUS4 enzyme activity by >65% (Purcell *et al*., 1998). Conversely, OE of *PKIN1* up-regulated the expression of *SUS4* and increased SUS4 enzyme activity by 20%–60% (McKibbin *et al*., 2006). In tomatoes and sweet potatoes, SnRK1 has been found to phosphorylate and inactivate sucrose phosphate synthase (SPS) (Liang *et al*., 2021; Ren *et al*., 2019; Wang *et al*., 2012), as well as trehalose 6-phosphate synthase (TPS) in *A. thaliana* (Halford and Hey, 2009; Polge and Thomas, 2007). In potatoes, SnRK1 protein kinase is required for the redox modulation of ADP-glucose pyrophosphorylase (AGPase) (Tiessen *et al*., 2003), the first rate-limiting enzyme in starch synthesis. Together, these results demonstrate that SnRK1 may be an important kinase that regulates sucrose metabolism and starch synthesis in wheat grains. Therefore, inhibition of *TPS* and *SUS* by *TaWUS-like-5D* may also be dependent on SnRK1 activity in a potential feedback mechanism. Further research should be conducted to explore this possibility.

In conclusion, *TaWUS-like-5D* was found to inhibit *SUS* and *TPS* transcription, thereby sharply decreasing starch synthesis in wheat grains. As a *WUS* family member, *TaWUS-like-5D* negatively regulates TKW and wheat yield. Based on our results, *TaWUS-like-5D* could be used to improve wheat grain yield through genetic engineering. This study improves our understanding of the functions of *WUS* family members in regulating plant growth and development and also provides a molecular basis for further elucidating the mechanism of *Wox*-mediated regulation of grain development in crops.

Methods

Plant materials and phenotype evaluation

The 716 F_2 lines used in BSA were derived from 2840 F_2 individuals of the bi-parental population produced from a cross between the 'Zhongyou9507' cultivar and the 'Hongjinmai' landrace (Table S2b). Wheat plants were cultivated in fields located in Shunyi (116°43′ E, 40°09′ N), Beijing, China, between 2016–2017 and 2018–2019. Wheat plants were cultivated under conventional irrigation and fertilization management practices. The *TaWUS-like-5D* OE and RNAi transgenic wheat lines (T_7–T_9; 5–7 independent transgenic lines, with 80 individuals per line), the CRISPR/Cas9-mediated *TaWUS-like* edited wheat lines *CriTaWUS-like-5A/5B/5D* (at least 20 individuals per edit) and the *TaWUS-like* kronos mutants *KTaWUS-like-5A/5B* (10 individuals per mutation) were cultivated in the Shunyi transgenic fields under the same conditions described above. Targeted genomic variations were detected through PCR and sequencing. The planting program was carried out as described by Su *et al*. (2011) and Si *et al*. (2021). The average temperature during the growing seasons was 10–22 °C.

Representatives of the homozygous transgenic OE and RNAi lines, *KTaWUS-likes* (self-pollinated to M_3), *CriTaWUS-likes* mutants (T_3–T_4 generations), as well as WT individuals, were selected to investigate a panel of agronomic traits. Phenotypic traits included TKW, GN, PH, heading date (HD), maturity date (MD), spikelet number per spike (SLN), spike length (SL), effective tiller number/spike number (TN/SN), GT, GW and GL. All traits were measured as described by Liu *et al*. (2023).

Transgene vector construction and wheat transformation

The full-length *TaWUS-like-5D* cDNA (969 bp) was amplified and sequentially cloned into the pWMB110 vector (*Bam*HI/*Eco*RI sites) to obtain the *TaWUS-like-5D* OE construct. To obtain the *TaWUS-like-5D*-RNAi construct, a 200-bp fragment derived from the *TaWUS-like-5D* cDNA (465–664 nucleotides) was amplified and sequentially cloned into the pAHC-PSK vector at the *Spe*I/*Eco*RV and *Hpa*I/*Sac*I sites in opposite directions, with an intron between them to create a hairpin structure. The single guide RNA (sgRNA) sequences were designed to target a conserved region in the first exon of *TaWUS-likes*. Finally, fragments of the active TaW5-sgRNA3 were amplified and inserted into CRISPR/Cas9 vector pJIT163-2NLSCas9 to obtain the fused expression vector pU6-TaW5-sgRNA3. This construct was used to edit *TaWUS-like-5A/5B/5D* and generate the *CriTaWUS-likes* lines. All constructs (OE/RNAi/CRISPR/Cas9) were transformed into immature embryos of the wheat cultivar 'KN199' using *Agrobacterium*-mediated transformation as described in Wang *et al*. (2017) and Wang *et al*. (2014b). All primers are listed in Table S3a,b.

RNA isolation, reverse transcription and qRT-PCR

Total RNA was isolated from leaf, stem, root and grain tissues using TIANGEN RNA Extraction Kits (Tiangen, Beijing, China). Approximately 2 μg of total RNA was reverse transcribed into cDNA using the SuperScript III RT system (Invitrogen, Madison, WI, USA), according to the manufacturer's instructions. qRT-PCR was performed as described by Liu *et al*. (2023) on an Applied

Biosystems 7500 Real-time PCR system (Thermo Fisher, USA), using *actin* as the housekeeping gene. All primers are listed in Table S4.

RNA-Seq analysis

Total RNA was extracted at 10 DPA from the wheat grains of three *TaWUS-like*-OE lines and WT plants using TIANGEN RNA Extraction kits, according to the manufacturer's instructions. The cDNA library was constructed and paired-end sequenced on an Illumina HiSeq 2500 platform (Illumina, San Diego, CA, USA) at BaiXu Biotechnology Company (Beijing, China). Clean reads were mapped to the CS wheat reference genome (IWGSCv1.0). Transcriptomic analysis was performed in Edge R (1.3.1093.0) according to the method of Chi *et al*. (2019). DEGs (Fold Change ≥2 and False Discovery Rate <0.01) were retained as fragments per kilobase per million reads (FPKM). DEG transcription levels were used to develop cluster heat maps (Table S5). Each sample consisted of three biological replicates.

DNA library construction and whole-genome sequence of bulked DNA

Leaf samples of 32 individuals derived from F_2 bi-parental progeny with extremely differential TKW traits (TKW ≥58 g or <28 g) were utilized for BSA and pooled in equal amounts to obtain the highest bulks (CH) and the lowest bulks (CL), respectively. DNA was extracted from the two parents and two bulks using the cetyltrimethyl ammonium bromide (CTAB) method according to standard protocols. DNA degradation and contamination were monitored on 1% agarose gels, and DNA purity was evaluated using a NanoPhotometer Spectrophotometer (IMPLEN, CA, USA). DNA concentration was measured using Qubit DNA Assay Kits in a Qubit 2.0 Fluorometer (Life Technologies, CA, USA). DNA libraries were constructed using Truseq Nano DNA HT Sample preparation Kits (Illumina, San Diego, CA, USA), according to the manufacturer's instructions. Paired-end sequencing was performed separately on an Illumina Hiseq XTen sequencer (Illumina, San Diego, CA, USA) at Smartgenomics Technology Institute (Tianjin, China).

Clean reads (Table S1) were assembled and aligned (RefSeq V2.1) to the CS wheat reference genome released from the International Wheat Genome Sequencing Consortium (IWGSC) in 2018 (Appels *et al*., 2018). SNP and InDel variant calling was performed using the Unified Genotyper function in GATK (McKenna *et al*., 2010). The PL genotype was used as the reference to standardize the CH and CL genotype and to calculate their SNP-index. The SNP-index was calculated using all SNP positions except those with SNP-index <0.3 and read depth <7, as these may represent spurious SNPs called due to sequencing and/or alignment errors. The delta SNP/InDel index was calculated as the SNP-index of the CH bulk subtracted from the SNP-index of the CL bulk. The sliding window method was used to obtain the SNP/InDel index of the whole genome, using a window size of 1 Mb and an increment of 10 kb. The SNP-index graphs for the CH and CL bulks, as well as the corresponding Δ (SNP-index) CH-CL graph, were constructed, and the statistical confidence intervals of Δ (SNP-index) were estimated, using read depths under the null hypothesis of no QTLs. For each read depth, the 95% or 99% confidence intervals of Δ (SNP-index) were obtained according to the method of Takagi *et al*. (2013).

Protein sequence alignment and phylogenetic analysis of Wox proteins

Wheat, rice, *A. thaliana*, and maize Wox protein sequences were retrieved from the Ensemble Plants database (http://plants.ensembl.org/) and aligned using Clustal X. The neighbour-joining (N-J) phylogenetic tree was constructed with 1000 bootstrap replicates using MEGA7.0 (V7.0.26). The TaWUS-like homoeologous protein sequences were aligned using DNAMAN (Lynnon Biosoft, Quebec, Canada). All gene accession numbers are listed in Table S6.

Analysis of the *TaWUS-like* homoeologous haplotypes

Haps evolution was analysed using 387 tetraploid/hexaploid wheat accessions divided into four groups: wild emmer (n = 61), domesticated tetraploid (n = 98), hexaploid landrace (n = 140) and hexaploid cultivar (n = 88). The ancestral-*haps* (*aHaps*) were inferred by IntroBlocker as described by Wang *et al*. (2022), while the germplasm-based *haps* (*gHaps*) for each 1 Mb bin were inferred using ggComp as described by Yang *et al*. (2022), with default parameters. Finally, the Shannon diversity index of each group was calculated to determine the significance of the *haps* differences. *Haps* association analysis was conducted according to the method of Liu *et al*. (2023).

Y2H and LCI assays

The Y2H assay was performed as described previously (Wu and Li, 2017). The *TaWUS-like-5D* and *SnRK1-4B* coding sequences (CDSs) were amplified and sub-cloned into the *pGBKT7* and *pGADT7* vectors, respectively, to generate the *TaWUS-like-5D-BD* and *SnRK1-4B-AD* plasmids. After the co-transformation of both plasmids into 'AH109' yeast cells, interactions between the expressed proteins were evaluated by the growth of the co-transformants on a selection medium (SD/-Trp/-Leu/-His/-Ade). The Y2H assay was performed in accordance with the Yeast Protocols Handbook (Takara Bio, San Jose, CA, USA).

The LCI assay for the interaction between TaWUS-like-5D and SnRK1-4B was performed in *N. benthamiana* leaves as described previously (Liu *et al*., 2017). The full-length *TaWUS-like-5D* and *SnRK1-4B* CDSs were fused with the N-terminal and C-terminal regions of the luciferase (*LUC*) reporter gene, respectively, to form *nLUC-TaWUS-like-5D* and *SnRK1-4B-cLUC*, which were then transformed into *A. tumefaciens* 'GV3103'. Bacteria harbouring the nLUC and cLUC derivative constructs were co-infiltrated into *N. benthamiana*. LUC activity was photographed and analysed 48–72 h following infiltration using the Night SHADE LB 985 Plant Imaging System (Berthold Technologies, Germany).

BiFC assays

For BiFC assays, the coding sequences for N-terminal and C-terminal yellow fluorescence proteins (YFPs) were fused to the C-termini of the full-length *TaWUS-like-5D* and *SnRK1-4B* CDSs, respectively. *A. tumefaciens* 'GV3101' was transformed with either the experimental or control vector and then infiltrated into young leaves of *N. benthamiana*. Fluorescence signals were observed with confocal microscopy (LSM880; Carl Zeiss, Germany).

Determination of sugar, starch and protein content

Soluble carbohydrates (sucrose, glucose, fructose and trehalose) were extracted from 300 mg each of fresh leaves, grains and stems according to the method of Lunn *et al*. (2006). The content of each sugar was determined by high-performance liquid chromatography (HPLC) (Waters 600 Gradient Controller; Waters Corporation, Milford, MA, USA) with a NH_2 column (5 mL, 4.6 mm × 250 mm I.D.; Inertsil HPLC column; GL Sciences, Tokyo, Japan). HPLC was performed following the procedure described by Chang *et al*. (2013). Total starch and amylose were extracted from the endosperm and quantified following the Chinese National Standard for Cereals (NY/T11-1985, NY/T11-1987) using the optical rotation method. Protein content was measured using the near-infrared reflectance spectroscopy (DA 7200, Perten, Spring-field, IL, USA).

Determination of cellulose and lignin content

Dry mature grains were chopped and then milled (Tissuelyser-48; Qiagen, Beijing, China). The grain powder was sifted through 380-μm and 250-μm mesh screens, and the sieved powder was collected for further analysis. Near-infrared (NIR) spectra of the powder samples were acquired on a FOSS NIR Systems 5000 spectrometer (FOSS Analytics, Silver Spring, MD, USA), according to the method of Li *et al*. (2015). Winscan v1.50 was used for spectral measurement and analysis. The cellulose and lignin contents were determined according to the method of Soest and Wine (1967). Precisely, 0.50 g of powder was used for chemical analyses. All analyses used analytical grade reagents. Cellulose and lignin standards were obtained from Sigma-Aldrich (Burlington, MA, USA). The relative error of the five technical replicates of each sample was controlled at <5%.

Determination of phytohormone levels

Phytohormone levels were determined in wheat grains at 10 DPA and uppermost stems at the heading stage for *TaWUS-like*-5D OE lines and WT plants. Sample extraction and enrichment were performed according to the method of Si *et al*. (2021). Phytohormone levels were determined using ultra-high-performance liquid chromatography–mass spectroscopy (UHPLC–MS) (Vanquish; Thermo Fisher, USA) with an HSS T3 column (50 × 2.1 mm, 1.8 μm; Waters Corporation, Milford, MA, USA). UHPLC–MS was performed according to the methods of Si *et al*. (2021) and Yi (2016). Purified 99% standards of CTK, ABA, IAA, brassinolide (BR), GA_3 and GA_4 were obtained from Sigma-Aldrich (Burlington, MA, USA). Each sample consisted of at least three biological repeats.

Statistical analysis

One-way analysis of variance (ANOVA) and Tukey's multiple comparison test were performed to determine statistical significance (*$P < 0.05$; **$P < 0.01$; and ***$P < 0.001$). Statistical analysis was performed using SPSS 16.0. A two-tailed Hutcheson *t*-test (Hutcheson, 1970) was utilized to determine statistically significant differences in the Shannon diversity index values between groups. All experiments were performed using no less than three replicates per sample. Data are presented as the mean values ± standard deviations (STDEV).

Acknowledgements

This study was supported by the National Key Research and Development Program of China (2023YFF1000600 to HXL, 2016YFD0100402 to HXL), Biological Breeding-National Science and Technology Major Project (2023ZD0406802), which supported by the Ministry of Agriculture and Rural Affairs (MARA), the National Natural Science Foundation of China (31471492 to HXL) and the CAAS-Innovation Program (HXL). We are grateful to Researcher J. Q. Sun (Institute of Crop Sciences, CAAS, China) for his critical review of this manuscript.

Conflict of interest

The authors declare no competing interests.

Author contributions

H.X.L conceived the whole project, performed most of the experiments, and wrote and revised the manuscript; J.H and X.M.S. constructed the F_2 segregation population and performed phenotype evaluation and genotype verification; X.T.Y., J.H and T.L performed LCI, EMSA and transcriptomic analysis; Y.Q.W. and S.Ur R. fine-mapped the QTL and performed genotyping; L.Z. and C.Y.H. assisted in BSR sequencing and data analysis; W.L.G conducted the analysis of haplotype domestication and polyploidization; H.X.L and Y.Q.W. developed the transgenic and CRISPR/Cas9-edited lines and performed the wheat transformation; C.Y.H, W.L.G and X.Y.Z provided experimental advice and revised the manuscript; all authors have read and approved the manuscript.

Data availability statement

The data that supports the findings of this study are available in the supplementary material of this article.

References

Appels, R., Eversole, K., Stein, N. and Feuillet, C. (2018) Shifting the limits in wheat research and breeding using a fully annotated reference genome. *Science* **361**, aar7191.

Baena-González, E., Rolland, F., Thevelein, J.M. and Sheen, J. (2007) A central integrator of transcription networks in plant stress and energy signaling. *Nature* **448**, 938–942.

Baud, S., Vaultier, M.N. and Rochat, C. (2004) Structure and expression profile of the sucrose synthase multigene family in *Arabidopsis*. *J. Exp. Bot.* **55**, 397–409.

Broeckx, T., Hulsmans, S. and Rolland, F. (2016) The plant energy sensor: evolutionary conservation and divergence of SnRK1 structure, regulation, and function. *J. Exp. Bot.* **67**, 6215–6252.

Carlson, S.J., Chourey, P.S., Helentjaris, T. and Dattaet, R. (2002) Gene expression studies on developing kernels of maize sucrose synthase (SuSy) mutants show evidence for a third *SuSy* gene. *Plant Mol. Biol.* **49**, 15–29.

Chang, Q., Liu, J., Wang, Q.L. and Han, L.N. (2013) The effect of *Puccinia striiformis* f. sp. *tritici* on the levels of water-soluble carbohydrates and the photosynthetic rate in wheat leaves. *Physiol. Mol. Plant Pathol.* **84**, 131–137.

Chevalier, P. and Lingle, S.E. (1983) Sugar metabolism in developing kernels of wheat and barley. *Crop Sci.* **23**, 272–277.

Chi, Q., Guo, L.J., Ma, M., Zhang, L.J., Mao, H.D., Wu, B.W., Liu, X.L. *et al*. (2019) Global transcriptome analysis uncovers the gene co-expression regulation network and key genes involved in grain development of wheat (*Triticum aestivum* L.). *Funct. Integr. Genomics* **19**, 853–866.

Cho, S.H., Yoo, S.C., Zhang, H., Pandeya, D., Koh, H.J., Hwang, J.Y., Kim, G.T. *et al*. (2013) The rice narrow *leaf2* and narrow *leaf3* loci encode *WUSCHEL*-related homeobox 3A (*OsWOX3A*) and function in leaf, spikelet, tiller and lateral root development. *New Phytol.* **198**, 1071–1084.

Chourey, P.S. and Nelson, O.E. (1976) The enzymatic deficiency conditioned by the *shrunken-1* mutation in maize. *Biochem. Genet.* **14**, 1041–1055.

Chourey, P.S., Taliercio, E.W., Carlson, S.J. and Ruan, Y.L. (1998) Genetic evidence that the two isozymes of sucrose synthase present in developing maize endosperm are critical, one for cell wall integrity and the other for starch biosynthesis. *Mol. Gen. Genet.* **259**, 88–96.

Counce, P.A. and Gravois, K.A. (2006) Sucrose synthase activity as a potential indicator of high rice grain yield. *Crop Sci.* **46**, 1501–1507.

Dong, L., Wang, F.M., Liu, T., Dong, Z.Y., Li, A.L., Jing, R.L., Mao, L. *et al*. (2014) Natural variation of *TaGASR7-A1* affects grain length in common wheat under multiple cultivation conditions. *Mol. Breed.* **34**(3), 937–947.

Fallahi, H., Scofield, G.N., Badger, M.R., Chow, W.S., Furbank, R.T. and Ruan, Y.L. (2008) Localization of sucrose synthase in developing seed and siliques of *Arabidopsis thaliana* reveals diverse roles for *SUS* during development. *J. Exp. Bot.* **59**, 3283–3295.

Figueroa, C. and Lunn, J. (2016) A tale of two sugars: trehalose 6-phosphate and sucrose. *Plant Physiol.* **172**(1), 7–27.

Gao, Y.J., An, K.X., Guo, W.W., Chen, Y.M., Zhang, R.J., Zhang, X., Chang, S.Y. *et al*. (2021) The endosperm-specific transcription factor *TaNAC019* regulates glutenin and starch accumulation and its elite allele improves wheat grain quality. *Plant Cell* **33**(3), 603–622.

Gao, Y.J., Li, Y.S., Xia, W.Y., Dai, M.Q., Dai, Y., Wang, Y.G., Ma, H.G. *et al*. (2023) The regulation of grain weight in wheat. *Seed Biol.* **2**, 17.

Ge, H.M., You, G.X., Wang, L.F., Hao, C.Y., Dong, Y.C., Li, Z.S. and Zhang, X.Y. (2012) Genome selection sweep and association analysis shed light on future breeding by design in wheat. *Crop Sci.* **52**, 1218–1228.

Gegas, V., Nazari, A., Griffiths, S., Simmonds, J., Fish, L., Orford, S., Sayers, L. *et al*. (2010) A genetic framework for grain size and shape variation in wheat. *Plant Cell* **22**(4), 1046–1056.

Gehring, W.J., Müller, M., Affolter, M., Percival-Smith, A., Billeter, M., Qian, Y.Q., Otting, G. *et al*. (1990) The structure of the homeodomain and its functional implications. *Trends Genet.* **6**, 323–329.

Godfray, H.C., Beddington, J.R., Crute, I.R., Haddad, L., Lawrence, D., Muir, J.F., Pretty, J. *et al*. (2010) Food security: the challenge of feeding 9 billion people. *Science* **327**(5967), 812–818.

Gonzali, S., Novi, G., Loreti, E., Paolicchi, F., Poggi, A., Alpi, A. and Perataet, P. (2005) A turanose-insensitive mutant suggests a role for *WOX5* in auxin homeostasis in *Arabidopsis thaliana*. *Plant J.* **44**(4), 633–645.

van der Graaff, E., Laux, T. and Rensing, S.A. (2009) The *WUS* homeobox containing (*WOX*) protein family. *Genome Biol.* **10**, 248.

Haecker, A., Gross-Hardt, R., Geiges, B., Sarkar, A., Breuninger, H., Herrmann, M. and Laux, T. (2004) Expression dynamics of *WOX* genes mark cell fate decisions during early embryonic patterning in *Arabidopsis thaliana*. *Development* **131**, 657–668.

Halford, N.G. and Hey, S.J. (2009) Snf1-related protein kinases (SnRKs) act within an intricate network that links metabolic and stress signaling in plants. *Biochem. J.* **419**, 247–259.

Halford, N.G. and Paul, M.L. (2003) Carbon metabolite sensing and signaling. *Plant Biotechnol. J.* **1**, 381–398.

Hao, Q., Zhang, L., Yang, Y., Shan, Z. and Zhou, X.A. (2019) Genome-wide analysis of the *WOX* gene family and function exploration of *GmWOX18* in soybean. *Plan. Theory* **8**, 215.

Hirose, T., Scofield, G.N. and Terao, T. (2008) An expression analysis profile for the entire sucrose synthase gene family in rice. *Plant Sci.* **174**, 534–543.

Hou, J., Jiang, Q.Y., Hao, C.Y., Wang, Y.Q., Zhang, H.N. and Zhang, X.Y. (2014) Global selection on sucrose synthase haplotypes during a century of wheat breeding. *Plant Physiol.* **164**(4), 1918–1929.

Housley, T.L., Kirkeis, A.W., Ohm, H.W. and Patterson, F.L. (1981) An evaluation of seed growth in soft red winter wheat. *Can. J. Plant Sci.* **61**, 525–534.

Hurkman, W.J., McCue, K.F., Altenbach, S.B., Korn, A., Tanaka, C.K., Kotharia, K.M., Johnson, E.L. *et al*. (2003) Effect of temperature on expression of genes encoding enzymes for starch biosynthesis in developing wheat endosperm. *Plant Sci.* **164**, 873–881.

Hutcheson, K. (1970) A test for comparing diversities based on the Shannon formula. *J. Theor. Biol.* **29**, 151–154.

Jha, P., Ochatt, S.J. and Kumar, V. (2020) WUSCHEL: a master regulator in plant growth signaling. *Plant Cell Rep.* **39**, 431–444.

Jia, M.L., Li, Y.N., Wang, Z.Y., Tao, S., Sun, G.L., Kong, X.C., Wang, K. *et al*. (2021) TaIAA21 represses TaARF25-mediated expression of *TaERFs* required for grain size and weight development in wheat. *Plant J.* **108**(6), 1754–1767.

Jiang, Q.Y., Hou, J., Hao, C.Y., Wang, L.F., Ge, H.M., Dong, Y.S. and Zhang, X.Y. (2011) The wheat (*T. aestivum*) *sucrose synthase 2* gene (*TaSus2*) active in endosperm development is associated with yield traits. *Funct. Integr. Genomics* **11**(1), 49–61.

Kato, T. (1995) Change of sucrose synthase activity in developing endosperm of rice cultivars. *Crop Sci.* **35**, 827–831.

Kumar, R. and Singh, R. (1980) The relationship of starch metabolism to grain size in wheat. *Phytochemistry* **19**, 2299–2303.

Laughon, A. (1991) DNA binding specificity of homeodomains. *Biochemistry* **30**, 11357–11367.

Laux, T., Mayer, K.F., Berger, J. and Jurgens, G. (1996) The *WUSCHEL* gene is required for shoot and floral meristem integrity in *Arabidopsis*. *Development* **122**, 87–96.

Leibfried, A., To, J.P.C., Busch, W., Stehling, S., Kehle, A., Demar, M., Kieber, J.J. *et al*. (2005) *WUSCHEL* controls meristem function by direct regulation of cytokinin-inducible response regulators. *Nature* **438**(7071), 1172–1175.

Li, X.L., Sun, C.J., Zhou, B.X. and He, Y. (2015) Determination of hemicellulose, cellulose and lignin in *Moso Bamboo* by near infrared spectroscopy. *Sci. Rep.* **5**(1), 17210.

Li, N., Xu, R., Duan, P. and Li, Y.H. (2018) Control of grain size in rice. *Plant Reproduction* **31**(3), 237–251.

Li, Z., Liu, D., Xia, Y., Li, Z.L., Jing, D.D., Du, J.J., Niu, N. *et al*. (2020) Identification of the *WUSCHEL*-related homeobox (*WOX*) gene family, and interaction and functional analysis of *TaWOX9* and *TaWUS* in Wheat. *Int. J. Mol. Sci.* **21**(5), 1581.

Liang, J., Zhang, S., Yu, W., Wu, X., Wang, W., Peng, F. and Xiao, Y. (2021) PpSnRK1α overexpression alters the response to light and affects photosynthesis and carbon metabolism in tomato. *Physiol. Plant.* **173**, 1808–1823.

Liu, J., Cheng, X., Liu, P. and Sun, J. (2017) miR156-targeted SBP-box transcription factors interact with DWARF53 to regulate *TEOSINTE BRANCHED1* and *BARREN STALK1* expression in bread wheat. *Plant Physiol.* **174**, 1931–1948.

Liu, H.X., Si, X.M., Wang, Z.Y., Cao, L.Y., Gao, L.F., Zhou, X.L., Wang, W.X. *et al*. (2023) *TaTPP-7A* positively feedback regulates grain filling and wheat yield through T6P-SnRK1 signaling pathway and sugar-ABA interaction. *Plant Biotechnol. J.* **21**, 1159–1175.

Lunn, J.E., Feil, R., Hendriks, J.H.N., Gibon, Y., Morcuende, R., Osuna, D., Scheible, W. *et al*. (2006) Sugar-induced increases in trehalose 6-phosphate are correlated with redox activation of ADP-glucose pyrophosphorylase and higher rates of starch synthesis in *Arabidopsis thaliana*. *Biochem. J.* **397**, 139–148.

Mao, H.D., Jian, C., Cheng, X.X., Chen, B., Mei, F.M., Li, F.F., Zhang, Y.F. *et al*. (2022) The wheat ABA receptor gene *TaPYL1-1B* contributes to drought tolerance and grain yield by increasing water-use efficiency. *Plant Biotechnol. J.* **20**(5), 846–861.

Maraña, C., Garcla-Olmedo, F. and Carbonero, P. (1988) Linked sucrose synthase genes in group-7 chromosomes in hexaploid wheat (*Triticum aestivum* L.). *Gene* **63**(2), 253–260.

Martínez-Barajas, E., Delatte, T., Schluepmann, H., de Jong, G.J., Somsen, G.W., Nunes, C., Primavesi, L.F. *et al*. (2011) Wheat grain development is characterized by remarkable trehalose 6-phosphate accumulation pregrain filling: tissue distribution and relationship to SNF1-related protein kinase1 activity. *Plant Physiol.* **156**, 373–381.

Mayer, K.F., Schoof, H., Haecker, A., Lenhard, M., Jurgens, G. and Laux, T. (1998) Role of *WUSCHEL* in regulating stem cell fate in the *Arabidopsis* shoot meristem. *Cell* **95**, 805–815.

McKenna, A., Hanna, M., Banks, E., Sivachenko, A., Cibulskis, K., Kernytsky, A., Garimella, K. *et al*. (2010) The genome analysis toolkit: a mapReduce framework for analyzing next-generation DNA sequencing data. *Genome Res.* **20**, 1297–1303.

McKibbin, R.S., Muttucumaru, N., Paul, M.J., Powers, S.J., Burrell, M.M., Coates, S., Purcell, P.C. *et al*. (2006) Production of high-starch, low-glucose potatoes through over-expression of the metabolic regulator SnRK1. *Plant Biotechnol. J.* **4**, 409–418.

Nunes, C., O'Hara, L.E., Primavesi, L.F., Delatte, T.L., Schluepmann, H., Somsen, G.W., Silva, A.B. *et al*. (2013) The trehalose 6-phosphate/SnRK1 signaling

pathway primes growth recovery following relief of sink limitation. *Plant Physiol.* **162**(3), 1720–1732.
O'Hara, L., Paul, M. and Wingler, A. (2013) How do sugars regulate plant growth and development? New insight into the role of trehalose-6-phosphate. *Mol. Plant* **6**(2), 261–274.
Polge, C. and Thomas, M. (2007) SNF1/AMPK/SnRK1 kinases, global regulators at the heart of energy control? *Trends Plant Sci.* **12**, 20–28.
Purcell, P.C., Smith, A.M. and Halford, N.G. (1998) Antisense expression of a sucrose non-fermenting-1-related protein kinase sequence in potato results in decreased expression of sucrose synthase in tubers and loss of sucrose-inducibility of sucrose synthase transcripts in leaves. *Plant J.* **14**, 195–202.
Ren, Z., He, S., Zhao, N., Zhai, H. and Liu, Q. (2019) A sucrose non-fermenting-1-related protein kinase-1 gene, *IbSnRK1*, improves starch content, composition, granule size, degree of crystallinity and gelatinization in transgenic sweet potato. *Plant Biotechnol. J.* **17**, 21–32.
Ruan, Y.L., Llewellyn, D.J. and Furbank, R.T. (2003) Suppression of sucrose synthase gene expression represses cotton fiber cell initiation, elongation, and seed development. *Plant Cell* **15**, 952–964.
Sarkar, A.K., Luijten, M., Miyashima, S., Lenhard, M., Hashimoto, T., Nakajima, K., Scheres, B. *et al*. (2007) Conserved factors regulate signaling in *Arabidopsis thaliana* shoot and root stem cell organizers. *Nature* **446**, 811–814.
Shoaib, M., Yang, W.L., Shan, Q.Q., Sun, L.H., Wang, D.Z., Sajjad, M., Li, X. *et al*. (2020) TaCKX gene family, at large, is associated with thousand-grain weight and plant height in common wheat. *Theor. Appl. Genet.* **133**(11), 3151–3163.
Si, X.M., Wang, W.X., Wang, K., Liu, Y.C., Bai, J.P., Meng, Y.X., Zhang, X.Y. *et al*. (2021) A sheathed spike gene, *TaWUS-like* inhibits stem elongation in common wheat by regulating hormone levels. *Int. J. Mol. Sci.* **22**(20), 11210.
Skylar, A., Hong, F., Chory, J., Weigel, D. and Wu, X. (2010) STIMPY mediates cytokinin signaling during shoot meristem establishment in *Arabidopsis* seedlings. *Development* **137**, 541–549.
Van Soest, P.J. and Wine, R.H. (1967) Use of detergents in the analysis of fibrous feeds IV. determination of plant cell-wall constituents. *J. Assoc. Off. Anal. Chem.* **58**, 50–55.
Stein, O. and Granot, D. (2019) An overview of sucrose synthases in plants. *Front. Plant Sci.* **10**, 95.
Su, Z., Hao, C., Wang, L. and Dong, Y. (2011) Identification and development of a functional marker of *TaGW2* associated with grain weight in bread wheat (*Triticum aestivum* L.). *Theor. Appl. Genet.* **122**, 211–223.
Sun, J., Loboda, T., Sung, S.J. and Black, C.C. (1992) Sucrose synthase in wild tomato, *Lycopersicon chmielewskii*, and tomato fruit sink strength. *Plant Physiol.* **98**, 1163–1169.
Takagi, H., Abe, A., Yoshida, K., Kosugi, S., Natsume, S., Mitsuoka, C., Uemura, A. *et al*. (2013) QTL-seq: rapid mapping of quantitative trait loci in rice by whole genome resequencing of DNA from two bulked populations. *The Plant J.* **74**, 174–183.
Tang, G.Q. and Sturm, A. (1999) Antisense repression of sucrose synthase in carrot (*Daucus carota* L.) affects growth rather than sucrose partitioning. *Plant Mol. Biol.* **41**, 465–479.
Tang, L., He, Y., Liu, B., Xu, Y.Y. and Zhao, G.W. (2023) Genome-wide identification and characterization analysis of *WUSCHEL*-related homeobox family in melon (*Cucumis melo* L.). *Int. J. Mol. Sci.* **24**, 12326.
Tiessen, A., Prescha, K., Branscheid, A., Palacios, N., McKibbin, R., Halford, N.G. and Geigenberger, P. (2003) Evidence that SNF1-related kinase and hexokinase are involved in separate sugar-signaling pathways modulating posttranslational redox activation of ADP-glucose pyrophosphorylase in potato tubers. *Plant J.* **35**, 490–500.
Wang, X., Peng, F., Li, M., Yang, L. and Li, G. (2012) Expression of a heterologous SnRK1 in tomato increases carbon assimilation, nitrogen uptake and modifies fruit development. *J. Plant Physiol.* **169**, 1173–1182.
Wang, W., Li, G., Zhao, J., Chu, H., Lin, W., Zhang, D., Wang, Z. *et al*. (2014a) *Dwarf Tiller1*, a *Wuschel*-related homeobox transcription factor, is required for tiller growth in rice. *PLoS Genet.* **10**, e1004154.
Wang, Y., Cheng, X., Shan, Q. and Zhang, Y. (2014b) Simultaneous editing of three homoeoalleles in hexaploid bread wheat confers heritable resistance to *Powdery mildew*. *Nat. Biotechnol.* **32**, 947–951.
Wang, Y.Q., Hao, C.Y., Zheng, J., Ge, H.M., Zhou, Y., Ma, Z.Q. and Zhang, X.Y. (2015) A haplotype block associated with thousand-kernel weight on chromosome 5DS in common wheat (*Triticum aestivum* L.). *J. Integr. Plant Biol.* **8**, 662–672.
Wang, K., Liu, H., Du, L. and Ye, X. (2017) Generation of marker-free transgenic hexaploid wheat via an *Agrobacterium*-mediated co-transformation strategy in commercial Chinese wheat varieties. *Plant Biotechnol. J.* **15**, 614–623.
Wang, Z.H., Wang, W.X., Xie, X.M. and Wang, Y.F. (2022) Dispersed emergence and protracted domestication of polyploid wheat uncovered by mosaic ancestral haploblock inference. *Nat. Commun.* **13**(1), 3891.
Wingler, A., Delatte, T.L., O'Hara, L.E., Primavesi, L.F., Jhurreea, D., Paul, M.J. and Schluepmann, H. (2012) Trehalose 6-phosphate is required for the onset of leaf senescence associated with high carbon availability. *Plant Physiol.* **158**, 1241–1251.
Wu, X.Y. and Li, T. (2017) A Casein Kinase II phosphorylation site in AtYY1 affects its activity, stability, and function in the ABA response. *Front. Plant Sci.* **8**, 323.
Xu, S.M., Brill, E., Llewellyn, D.J., Furbank, R.T. and Ruan, Y.L. (2012) Overexpression of a potato sucrose synthase gene in cotton accelerates leaf expansion, reduces seed abortion, and enhances fiber production. *Mol. Plant* **5**, 430–441.
Yan, X., Zhao, L., Ren, Y., Dong, Z., Cui, D. and Chen, F. (2019) Genome-wide association study revealed that the *TaGW8* gene was associated with kernel size in Chinese bread wheat. *Sci. Rep.* **9**, 2702.
Yang, Z.Z., Wang, Z.H., Wang, W.X. and Xie, X.M. (2022) GGComp enables dissection of germplasm resources and construction of a multiscale germplasm network in wheat. *Plant Physiol.* **188**(4), 1950–1965.
Yi, Y. (2016) *Detection, preparation and utilization for the plant growth regulator from sargassum*. Fujian Agriculture and Forestry University. Thesis.
Yoshida, H., Okada, S., Wang, F., Shiota, S., Mori, M., Kawamura, M., Zhao, X. *et al*. (2023) Integrated genome-wide differentiation and association analyses identify causal genes underlying breeding-selected grain quality traits in japonica rice. *Mol. Plant* **16**, 1460–1477.
Zhang, X., Zong, J., Liu, J., Yin, J. and Zhang, D. (2010) Genome-wide analysis of *WOX* gene family in rice, sorghum, maize, *Arabidopsis* and poplar. *J. Integr. Plant Biol.* **52**, 1016–1026.
Zhang, D.D., Wang, B.N., Zhao, J.M., Zhao, X.B., Zhang, L.Q., Liu, D.C., Dong, L.L. *et al*. (2015) Divergence in homoeolog expression of the grain length-associated gene *GASR7* during wheat allohexaploidization. *Crop J.* **3**, 1–9.
Zhang, N., Yu, H., Yu, H., Cai, Y., Huang, L., Xu, C., Xiong, G. *et al*. (2018) A core regulatory pathway controlling rice tiller angle mediated by the *LAZY1*-dependent asymmetric distribution of auxin. *Plant Cell* **30**(7), 1461–1475.
Zrenner, R., Salanoubat, M., Willmitzer, L. and Sonnewald, U. (1995) Evidence of the crucial role of sucrose synthase for sink strength using transgenic potato plants (*Solanum tuberosum* L.). *Plant J.* **7**, 97–107.
Zuo, J. and Li, J. (2014) Molecular genetic dissection of quantitative trait loci regulating rice grain size. *Annu. Rev. Genet.* **48**, 99–118.

Supporting information

Additional supporting information may be found online in the Supporting Information section at the end of the article.

Figure S1 SNP variations and agronomic traits association analysis of the five candidate genes in 262 MCC.
Figure S2 Expression patterns of three *TaWUS-like* homologs in various CS wheat tissues at different developmental stages.
Figure S3 Nuclear localization of the TaWUS-like-5D TF.
Figure S4 Agronomic traits (a) and estimated grain yield (b) of transgenic lines and WT plants under field conditions.
Figure S5 Whole-plant and spike phenotypes of the transgenic and WT plants.
Figure S6 Tiller angles of the transgenic and WT plants under field conditions.

Figure S7 Identification and phenotypes of *CriTaWUS-likes* mutants (T_0).
Figure S8 Mutation schematic (a) and whole-plant agronomic trait evaluation (b) of *KTaWUS-like-5A/5B*.
Figure S9 Lemma and palea phenotypes of transgenic and WT plants.
Figure S10 Phenotypes of the transgenic *TaWUS-like-5D-OE* lines in *A. thaliana*.
Figure S11 Crude protein content in mature seeds of the transgenic wheat lines and WT plants.
Figure S12 Heat map of downstream genes of *TaWUS-likes* at 5, 15, and 20 DPA in wheat.
Figure S13 Heat map of downstream starch and protein regulatory genes of *TaWUS-likes* at 5 and 10 DPA.
Figure S14 Heat map of downstream starch and protein regulatory genes of *TaWUS-likes* at 15 and 20 DPA.

Table S1 Clean read statistics (1a and 1b) and Delta SNP/InDel index values at the physical locus (106–110 Mb) on chromosome 5DS (1c) used in BSA mapping.
Table S2 Agronomic traits and yields of transgenic and WT plants between 2016 and 2019 (2a); TKW and other agronomic traits of 716 F_2 segregation progeny used in BSR-seq (2b).
Table S3 Primers used to construct (3a) and confirm (3b) the transgenic OE lines, RNAi lines, and the *CriTaWUS-likes* and *KTaWUS-likes* mutants.
Table S4 Primers used to analyze the expression patterns of *TaWUS-likes*.
Table S5 RNA-seq heatmap data of *TaWUS-like-5D* OE lines and WT plants at 10, 5, 15, and 20 DPA.
Table S6 Accession numbers and annotations of *TaWUS-likes* homologous genes used in phylogenetic tree construction.